The Geographic Corridor for Rapid Climate Change in Southeast Europe and Ukraine

Bernhard Weninger and Thomas Harper

Introduction

One of the most significant discoveries of recent palaeoclimate research is the existence of a distinctly repetitive series of cooling anomalies that run through the entire Glacial into the Holocene period. Following the pioneering studies of P. Mayewski and E. Rohling, these cold anomalies are termed "Rapid Climate Change" (henceforth, RCC) events.[1] Since climate developments in the Glacial period are seldom referenced in archaeological studies that focus on the Holocene, but are nevertheless important for an understanding of the RCC mechanism, we begin our studies with a brief introduction to the climate records (oceanic and atmospheric) that are of major significance to our topic. The discovery some ten years ago that major cold periods could be caused by atmospheric circulation changes on a global scale, not only during the Glacial but also in the Holocene, was not entirely unexpected. Discoveries inevitably require considerable preparative work. This is certainly obvious for our present topic: the RCC mechanism, the discovery of which is perhaps best understood as the direct (and in retrospect indeed inevitable) outcome of one of the largest palaeoclimatological research programs yet to be undertaken – the Greenland Ice Sheet Project Two (henceforth, GISP2) deep drilling project.[2] Especially for the purposes of archaeological knowledge transfer, further details of GISP2 methodology are provided in a most informative manner in the Ice Chronicles.[3] Upon its completion in 1993, the GISP2 drilling had recovered one of the deepest (3053 m) ice cores in the Northern Hemisphere. This data is well-understood by researchers.[4] The stable oxygen isotope measurements ($\delta^{18}O$) from the GISP2 core (**Fig. 1,** above) provide compelling evidence that the Glacial was not a continuously cold period, as we may naively assume, but was in fact interrupted by a recurring sequence of warm periods (interstadials). Each of these interstadials has a rapid (decadal scale) onset, followed by a much slower – and often stepwise – return to stadial conditions.

Less commonly acknowledged, in comparison to the Greenland $\delta^{18}O$ record,[5] is the predictive power of a set of measurements on aerosols, dust particles, and wind-blown ions (such as Nitrate [NH_4], Sulphur Dioxide [SO_2], Calcium [Ca^{++}], and Chlorine [Cl^-]) that were processed in parallel to the $\delta^{18}O$ measurements.[6] This so-called glaciochemical data[7] includes, in particular, a long series of measurements on non-sea salt (nss) potassium ions, the concentration [K^+] of which was measured on ice samples from the same core. Figure 1 shows both data sets ($\delta^{18}O$ and nss [K^+]) in joint representation on the same time scale, recently revised[8] to allow for advances achieved in ice core age modelling. Whereas in general terms the $\delta^{18}O$ record can be taken as proxy for variations in North Atlantic air/ocean temperature, which are in turn related to changes in ocean circulation, the nss [K^+] measurements record the contemporary atmospheric dust flux (e. g. continental dust from northern Asia blown into the Greenland ice sheet). Importantly, as already recognised in the seminal publication of GISP2 glaciochemical data,[9] the Glacial and Holocene dust flux (including nss [K^+]) over the Greenland ice sheet is now more widely acknowledged as having a strong (causal) correlation with the strength of the Siberian High. Put together, the following results can be gleaned from the inverse relationship between $\delta^{18}O$ and nss [K^+] (**Fig. 1**; compare upper and lower parts): (1) the essentially warm and moist North Atlantic interstadials are characterised by major oceanic heat transport northwards from the equator, by way of the North Atlantic circulation in combination with a generally weak atmospheric circulation; and (2), the essentially cold and dry stadials are closely related to a reduction in North Atlantic deepwater formation, which leads to cooling in the North Atlantic in parallel with a general increase in the strength of Northern Hemispheric winds. Corresponding to their different interpretations, we therefore differentiate (if only as a convenient simplification) between an oceanic component of the climate system as represented by the GISP2 $\delta^{18}O$ record, and its atmospheric counterpart, the GISP2 nss [K^+] record.

Interestingly, as becomes clear from a closer look at **Figure 1** (below) in contrast to the oceanic cold ($\delta^{18}O$) intervals, the long series of atmos-

[1] Mayewski et al. 1997; Mayewski et al. 2004; Rohling et al. 2002; Rohling et al. 2009.
[2] GISP2 2012.
[3] Mayewski et al. 2002.
[4] GISP2 2012; with further references.
[5] First published in Grootes et al. 1993.
[6] Mayewski et al. 1997.
[7] See GISP2 2012 for a compilation of data.
[8] Vinther et al. 2006; Rasmussen et al. 2006, Svensson et al. 2006.
[9] Mayewski et al. 1997.

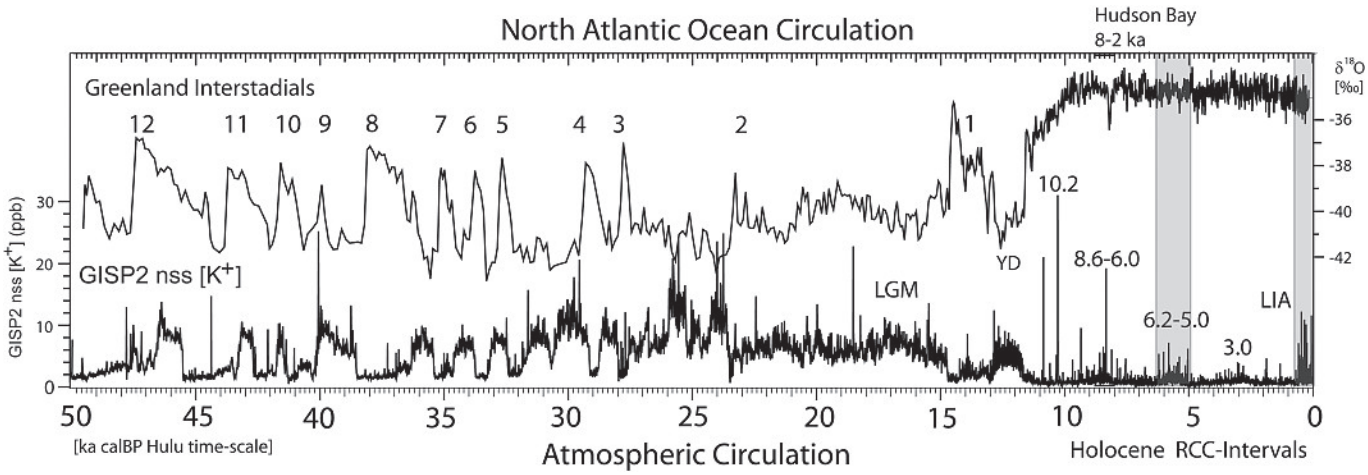

Fig. 1. High-resolution Greenland GISP2 ice core $\delta^{18}O$ record as a proxy for North Atlantic temperature (Grootes et al. 1993), shown together with GISP2 non-sea-salt potassium concentration (nss [K^+]; ppb) ion record as proxy for the strength of the Siberian High (Mayewski et al. 1997; Meeker/Mayewski 2002) in the time interval of 50–0 ka calBP. Below: Note the continuation of cold (RCC) conditions from the Glacial into the Holocene, as documented in the nss [K^+] record. Shaded regions: LIA (Little Ice Age and 6.2–5.0 ka calBP RCC interval). LGM = Late Glacial Maximum. GISP2 data are shown on the Hulu age model according to Weninger/Jöris 2008.

pheric cold periods (nss [K^+]) does not stop at the end of the Glacial. Following the transition from Glacial to Holocene (i. e. at the end of the Younger Dryas), the GISP2 $\delta^{18}O$ record indicates a largely stable North Atlantic circulation, with the major exception of the well-known 8.2–8.0 ka calBP event (Hudson Bay outflow). However, recent research[10] is becoming increasingly aware of the potential impact of the outflow of even smaller meltwater volumes into the North Atlantic prior to the Hudson Bay event, for example, along the St. Lawrence River at around 9.2 ka calBP.[11] In contrast to such oceanic events, the atmospheric (nss [K^+]) signature shows a series of cold events that run systematically (with repetitive occurrence every ~1450 years) throughout the entire extent of the Holocene, even up to modern times.[12] As indicated by shading in **Figure 1** (below), the most recent RCC is commonly referred to as the Little Ice Age (henceforth, LIA; ca. AD 1450–1929). The extent to which the oceanic 9.2 ka calBP event is related to the major nss [K^+] peak of similar age in the GISP2 record will be decided in future studies. According to Fleitmann et al.,[13] "the 'anomaly hunting' season for the 9.2 ka event [is] opened". As goes for the extended hunting-gathering-farming season, there is no reason why archaeologists should not participate in the RCC search.

To this purpose let us now study the GISP2 nss [K^+]) record in more detail for the Holocene period. Similar to the Glacial, the cold intervals that occur during the Holocene (which we term RCC events) are associated with an expansion and intensification of the Siberian High over northern Asia. Based on palaeoclimatological and environmental research undertaken during the last ten years, we now have at our disposal a steadily increasing number of records that demonstrate a notable impact of Holocene RCC anomalies upon terrestrial and marine systems at a variety of localities in the eastern Mediterranean.[14] It is becoming increasingly apparent that we may expect perhaps the most extreme RCC conditions during the period of 8.6–8.0 ka calBP, with particularly harsh conditions towards the end of this period (8.2–8.0 ka calBP). This would be due to the cumulative effects of RCC and the outflow of large amounts of Glacial meltwater from the Hudson Bay into the North Atlantic. We note *en passant* that, unfortunately, as demonstrated by Rohling and Pälike,[15] researchers sometimes still confuse the impacts of (atmospheric) RCC conditions with the consequences of the (oceanic) Hudson Bay outflow. From an archaeological perspective, it is important to note that these two events do indeed reinforce each other. Nevertheless, due to their widely different (centennial-scale) dating, we must clearly differentiate between the two mechanisms.[16]

Rather more demanding than the identification of the archaeological relevance of the 8.6–8.0 ka calBP RCC, which is omnipresent in eastern Mediterranean climate records,[17] is the question of whether the other major RCC intervals (e. g. ~10.2 ka calBP; ~9.3 ka calBP; ~6.2–5.0 ka calBP; ~3.0 ka calBP) that can be distinguished in GISP2 nss [K^+] are also correlated with synchronous changes occurring in prehistoric cultural systems. From a palaeoclimatological perspective, the present lack of archaeological substantiation for these events is likely not due to non-existing impact, but rather due to the lack of dedicated prehistoric studies. In this paper we

[10] E.g. Fleitmann et al. 2008.
[11] Cf. Yu et al. 2010; Lang et al. 2010.
[12] Mayewski et al. 1997; 2004)
[13] Fleitmann et al. 2008.
[14] E.g. Feurdean et al. 2008; Marino et al. 2009; Pross et al. 2009.
[15] Rohling/Pälike 2005.
[16] Clare/Weninger 2010.
[17] For a recent compilation, see Weninger/Clare 2009.

address whether it is possible to identify the societal impact of RCC conditions, as is forecasted in the GISP2 nss [K^+] record, with special attention given to the 6.2–5.0 ka calBP interval. In order to optimize the outcome of such an exploratory search to the maximum, our previous studies have focussed on available archaeological data for Greece, Bulgaria, Romania and Turkey.[18] For reasons to be presented in the following section, during the 6.2–5.0 ka calBP interval these studies are now extended to cover Ukraine.

The geographic corridor for RCC: modern analogues

Of particular interest for RCC-related studies in climate archaeology are two specific observations, namely: (1) the RCC cold anomalies have a pronounced seasonal character, with outbreaks of cold polar air occurring only a few days during winter and spring; and (2) the cold air outbreaks quite often follow the same path. We term this path the "Geographic Corridor (henceforth, GC)." The GC for RCC extends from northern Asia through the northern Pontic steppe regions (Ukraine), then runs through the Lower Danube (Romania), and from there into northern Greece. Following orographic channels through the Balkans, the cold winds then proceed southwards across the Aegean Sea.[19] After reaching the northern coast of Crete, the air flow is then channelled in an easterly direction towards the Levant and westwards along the southern periphery of the Peloponnese. We have compiled this description of the GC for RCC from a meteorological satellite video that shows a recent cold air outbreak (centred on a few days around January 31, 2012), when an anticyclone developing over the Black Sea pumped large amounts of cold air into the eastern Mediterranean. This remarkably detailed (potential) modern analogue for LIA/RCC conditions in the Black Sea littoral and adjoining regions, and in particular for Southeast Europe and the Aegean, is available from the website of WetterOnline.[20]

As can be recognised from this satellite film, we have little reason to doubt that during prehistoric periods the cold RCC winds would also have adhered to the corridor as described above. Intriguingly, these cold air masses also intrude into Thessaly. In comparison, the western regions of Greece appear to be sheltered to some extent by the central Greek mountain range, a situation also observed for southern Crete. Generally milder conditions are to be expected for the coastal regions; for example, the bay of Volos and maritime western Turkey. Such geographically detailed observations, helpful as they may be for archaeological RCC impact modelling, naturally require independent confirmation.

In assembling our results, we may not only infer a particularly high frequency of RCC conditions during the temporal intervals specified above, but further that – based on modern meteorological analogues – the circumpontic regions, Romania, Bulgaria and eastern Greece (including Thessaly and northern Crete) must have also in certain prehistoric periods been regularly subjected to anomalously cold spells. These persisted for short periods of time (a few days to two weeks), but brought with them extremely cold air masses with typical temperatures of approximately -40 °C. As documented in marine core LC21 (east of Crete), these air masses are capable of cooling the ocean surface temperature in the eastern Mediterranean, in a water column approximately 200 m in depth, within very few days.[21]

The geographic corridor for RCC: Southeast Europe and Ukraine

Looking to the meteorological conditions that lead to RCC conditions on broader geographic scales, it appears that there are actually two geographic corridors for the outflow of cold masses from the polar regions during times of pronounced Siberian High.[22] As shown in **Figure 2**, the first corridor runs east of the Himalayas across China and then continues into the Pacific. For this (eastern) corridor there are presently no studies on the archaeological impacts of RCC. The second (western) corridor also begins in Central Asia, but runs north of the Himalayas in a westerly direction, crossing the northern Pontic steppe into Ukraine before heading into Southeast Europe.

Building on results achieved in previous papers,[23] we therefore now extend our archaeological RCC studies to cover the 6.2–5.0 ka calBP interval in Ukraine. Again, the first step is to attain an overview of the cultural chronology in this region. In the following, we first provide a review of the radiocarbon chronology for the RCC study window in Greece, Bulgaria and Romania. For this review purpose, the ^{14}C data is presented in multi-group diagrams showing the major ^{14}C-dated Neolithic, Chalcolithic and Early

[18] Weninger et al. 2009; Clare et al. 2008; Clare/Weninger 2010.
[19] Rohling et al. 2002.
[20] WetterOnline 2012.
[21] Rohling et al. 2002.
[22] E.g. Saaroni et al. 1996; Sahsamanoglou et al. 1991; most recently: Tubi/Dayan 2012; with further references.
[23] Weninger et al. 2006; Weninger et al. 2009; Weninger et al. 2011; Clare 2013.

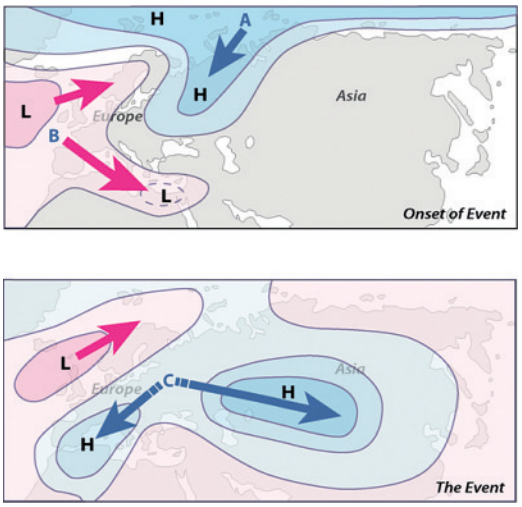

Fig. 2. Schematic representation of the synoptic atmospheric conditions that favour bitter cold air outbreaks from the polar regions during times of pronounced Siberian High. Note the existence of two corridors for cold air flow in the lower portion: one in a westward direction across the Ukraine and into the Mediterranean, and another in an eastward direction, running from Central Asia across Mongolia and into China. Graph: Tubi (pers. comm. 2012).

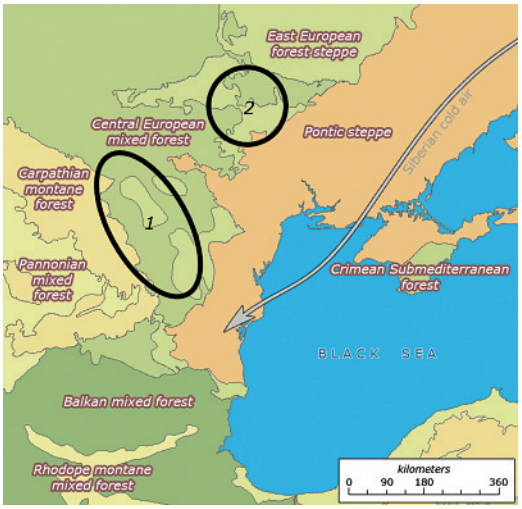

Fig. 3. Ecoregions along the Black Sea littoral (data from Olson et al. 2001). Winter cold air emanating from the Siberian High travels along this "steppe corridor" and can seriously affect the severity of regional weather conditions. 1 Nucleus of early Cucuteni-Tripolye settlement (Precucuteni A/Tripolye BI). 2 Main area of middle to late (Tripolye BII, CI, and CI–II) settlement in the Southern Bug-Dnieper interfluve, including giant-settlements.

Bronze Age sites. In the second section our focus is on the ^{14}C chronology for Ukraine, also during the RCC interval 6.2–5.0 ka calBP. For Ukraine, following the compilation of ^{14}C data, our main aim is to develop a chronological scheme, which conforms as accurately as possible to the site distributions for the different phases of Cucuteni-Tripolye as generalized by I. V. Manzura,[24] with the intention of facilitating further study into RCC impacts in this region (**Fig. 3**).

Radiocarbon calibration: time scales and methods

All archaeological chronologies constructed and discussed in this paper are based on tree ring-calibrated ^{14}C ages. For graphic representation of calibrated ^{14}C ages we use the method of 2-D dispersion calibration,[25] which has recently been shown to minimize the distortion produced by the nonlinearity of the ^{14}C age calibration curve based on quantum-theoretical considerations.[26] Numeric ages are given either on the Julian time scale with [calBC] units, or alternatively on the [calBP] time scale with 0 calBP equivalent to AD 1950. Calibrated age values are obtained using the CalPal software[27] and the INTCAL09 data set.[28] Note that, in this paper, we provide [calBP] ages for references to palaeoclimate data and [calBC] ages for archaeological data.

Radiocarbon calibration: ^{14}C database management

For radiocarbon calibration we use the CalPal software package,[29] which has recently been extended to support the management of large archaeological ^{14}C databases. For convenience in data management, the ^{14}C database is coded and stored in Excel® (xls) format. Presently, the largest CalPal database (Holocene Europe and the Near East) contains N=17.300 ^{14}C ages, each of which is coded as one line in the spreadsheet. The database allows for the entry/import of 12 variables altogether (Lab Code, ^{14}C Age, ^{14}C Std, δ^{13}C, Material, Species, Country, Period, Phase, Locus, Latitude, Longitude). In comparison to other ^{14}C databases, which are largely descriptive, CalPal is designed for rapid and convenient active (analytical) database management, both in terms of data import as well as graphic representation of results. This requires the implementation of a large number of filtering and screening routines, for which we have designed a new import dialogue (**Fig. 4**). With this dialogue, which calls directly on any CalPal-formatted xls database, it is possible to rapidly construct a graph that shows a maximum of 10 sets of calibrated probability distributions, each representing the ^{14}C data available. These sets could signify specific archaeological sites, a certain geographic region, a cultural phase or a given sample type. The necessary xls import/graphic output functions are implemented in CalPal with the help of Fortran calls that are implemented as subroutines in the Winteracter® library. In particular, for the purpose of Excel® database import/export through the Win® ODBC (Open Data Base Connectivity) interface, we have recently updated CalPal to make use of the new Winteracter® (version 8.2a) ODBC libraries. We note that the data tables (see Appendix, **Tables 1–27**) do not include calibrated ages, since these are automatically calculated during runtime.

[24] Manzura 2005.
[25] Weninger 1986.
[26] Weninger et al. 2011.
[27] Weninger/Jöris 2008.
[28] Reimer et al. 2009.
[29] Weninger/Jöris 2008.

Radiocarbon database

For the purposes of this study we have collated an extensive radiocarbon database for selected Neolithic, Chalcolithic (Eneolithic) and Early Bronze Age sites in Southeast Europe.[30] The integrated database contains N = 609 individual ^{14}C ages, which are compiled in **Tab. A** and the Appendix (**Tab. 1–26**), where they are arranged in order of country (Greece, Bulgaria, Romania) and according to archaeological sites.

A different representation is chosen for the ^{14}C data from the North Pontic region (Ukraine), in which case the ^{14}C data are arranged under the overall cultural heading "Cucuteni-Tripolye". It is important to note that in this paper we do not construct a site or phase-related ^{14}C chronology for Ukraine, as may be expected. Instead, the ^{14}C database (Appendix, **Tab. 27**) is compiled and analysed with the aim of providing absolute age intervals for each of the five Cucuteni-Tripolye site distribution maps published by Manzura.[31] To this aim, **Table 27** contains a reference for each ^{14}C age to one of the five Cucuteni-Tripolye maps (**Fig. 13 A–E**). The absolute age intervals for maps (**Fig. 13 A–E**) were calculated from summed calibrated probabilities shown in **Figure 12**. Note also that when compiling the Cucuteni-Tripolye ^{14}C database (**Tab. 27**) from the xls CalPal database, we have strongly screened and filtered the available data in order to create discrete (i. e. non-overlapping) periods which may be applied in demographic modelling.[32] Individual references for the Cucuteni-Tripolye ^{14}C data are provided in **Table 27**.

Southeast Europe: An Overview

In Southeast Europe the time interval 4200–3200 calBC corresponds to the transition from the Chalcolithic (or Copper Age, Final Neolithic, Eneolithic) to the Early Bronze Age. Unfortunately, the study of this transition is complicated due to the general lack of archaeological data, as well as regional differences in cultural terminology. Notwithstanding such terminological complications, common to most regions within the RCC corridor in Southeast Europe (Greece, Bulgaria, Romania) is an apparently abrupt transition from an agrarian to a more mobile pastoralist economy. This transition is most evident in the sudden and widespread abandonment of the many large multi-layer (floodplain-based) tell sites that are typical for the preceding Neolithic and Eneolithic/Chalcolithic periods. Around 4200 calBC the majority of the large magoules in northern Greece, including Thessaly as well as in Bulgaria were deserted. In these regions the abandonment of the tell settlements is accompanied with a distinct shift towards smaller mono-layer sites, including cave sites. In Greece the switch occurs with the onset of the so-called Final Neolithic (henceforth, FN). In Bulgaria, the corresponding period is known as the Transitional Period, which separates the Late Eneolithic from the Early Bronze Age. In the next sections, on the basis of ^{14}C dating and the mapping of site distributions for selected regions (Thessaly in Greece and the Lower Danube in Romania), we provide a review of the chronological and geographic extent of this switch in settlement patterns.

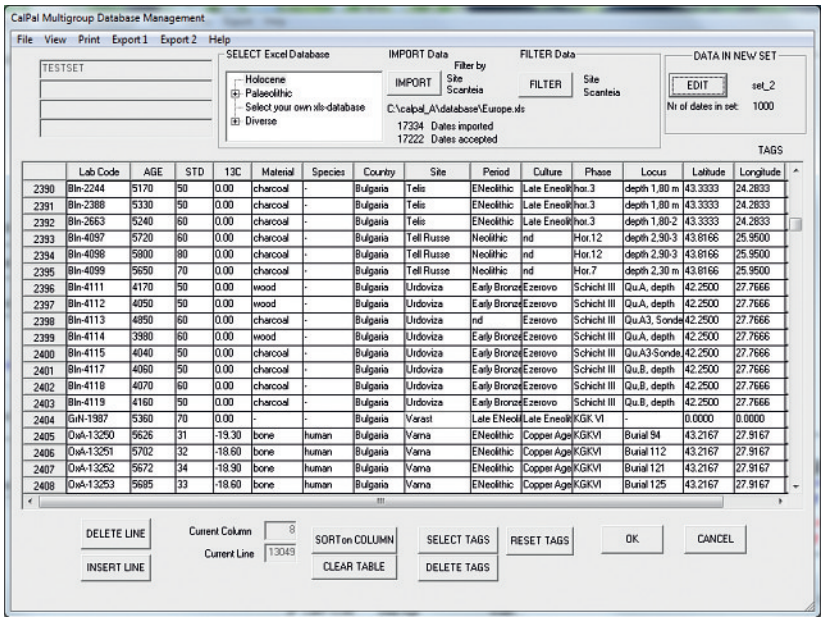

	Lab Code	AGE	STD	13C	Material	Species	Country	Site	Period	Culture	Phase	Locus	Latitude	Longitude
2390	Bln-2244	5170	50	0.00	charcoal	-	Bulgaria	Telis	ENeolithic	Late Eneolit	hor.3	depth 1,80 m	43.3333	24.2833
2391	Bln-2388	5330	50	0.00	charcoal	-	Bulgaria	Telis	ENeolithic	Late Eneolit	hor.3	depth 1,80 m	43.3333	24.2833
2392	Bln-2663	5240	60	0.00	charcoal	-	Bulgaria	Telis	ENeolithic	Late Eneolit	hor.3	depth 1,80-2	43.3333	24.2833
2393	Bln-4097	5720	60	0.00	charcoal	-	Bulgaria	Tell Russe	Neolithic	nd	Hor.12	depth 2,90-3	43.6166	25.9500
2394	Bln-4098	5800	80	0.00	charcoal	-	Bulgaria	Tell Russe	Neolithic	nd	Hor.12	depth 2,90-3	43.6166	25.9500
2395	Bln-4099	5650	70	0.00	charcoal	-	Bulgaria	Tell Russe	Neolithic	nd	Hor.7	depth 2,30 m	43.6166	25.9500
2396	Bln-4111	4170	50	0.00	wood	-	Bulgaria	Urdoviza	Early Bronze	Ezerovo	Schicht III	Qu.A, depth	42.2500	27.7666
2397	Bln-4112	4050	50	0.00	wood	-	Bulgaria	Urdoviza	Early Bronze	Ezerovo	Schicht III	Qu.A, depth	42.2500	27.7666
2398	Bln-4113	4850	60	0.00	charcoal	-	Bulgaria	Urdoviza	nd	Ezerovo	Schicht III	Qu.A3, Sonde	42.2500	27.7666
2399	Bln-4114	3980	60	0.00	wood	-	Bulgaria	Urdoviza	Early Bronze	Ezerovo	Schicht III	Qu.A, depth	42.2500	27.7666
2400	Bln-4115	4040	50	0.00	charcoal	-	Bulgaria	Urdoviza	Early Bronze	Ezerovo	Schicht III	Qu.A3-Sonde,	42.2500	27.7666
2401	Bln-4117	4060	50	0.00	charcoal	-	Bulgaria	Urdoviza	Early Bronze	Ezerovo	Schicht III	Qu.B, depth	42.2500	27.7666
2402	Bln-4118	4070	60	0.00	charcoal	-	Bulgaria	Urdoviza	Early Bronze	Ezerovo	Schicht III	Qu.B, depth	42.2500	27.7666
2403	Bln-4119	4160	50	0.00	charcoal	-	Bulgaria	Urdoviza	Early Bronze	Ezerovo	Schicht III	Qu.B, depth	42.2500	27.7666
2404	GrN-1987	5360	70	0.00	-	-	Bulgaria	Varast	Late ENeolit	Late Eneolit	KGK VI	-	0.0000	0.0000
2405	OxA-13250	5626	31	-19.30	bone	human	Bulgaria	Varna	ENeolithic	Copper Age	KGKVI	Burial 94	43.2167	27.9167
2406	OxA-13251	5702	32	-18.60	bone	human	Bulgaria	Varna	ENeolithic	Copper Age	KGKVI	Burial 112	43.2167	27.9167
2407	OxA-13252	5672	34	-18.90	bone	human	Bulgaria	Varna	ENeolithic	Copper Age	KGKVI	Burial 121	43.2167	27.9167
2408	OxA-13253	5685	33	-18.60	bone	human	Bulgaria	Varna	ENeolithic	Copper Age	KGKVI	Burial 125	43.2167	27.9167

*Fig. 4. Spreadsheet dialog (Win®OS) for ^{14}C database management. The dialog supports rapid filtering of requested variables by mouse-click. In practical application, the study data are first imported into the spreadsheet from an xls file, filtered within the dialog, and then exported into the CalPal multi-group menu to produce graphs of the type shown in **Figures 5; 7; 10; 12**.*

Greece

As a result of extensive archaeological surveys[33] and geomorphological studies[34], as well as diachronic analysis of prehistoric settlement patterns,[35] the fertile palaeo-floodplains of eastern Thessaly (Larissa plain) present one of the most extensively surveyed regions in Greece. It has recently been proposed that the often-noted lack of surface finds dating to the FN in Thessaly appears to have been caused by a drastic decline in population during this period.[36] Previous authors have argued that the general lack of FN pottery finds on Thessalian tells is due to destructive weathering.[37] However, by adding EBA

[30] The major sources for the ^{14}C dates used in this paper are Boyadziev 1995, Görsdorf/Bojadžiev 1996, László 1997, Lazarovici 2010 and Luca 2012.
[31] Manzura 2005.
[32] Harper 2013.
[33] Gallis 1992; Gallis 1994.
[34] van Andel et al. 1990; van Andel/Runnels 1995; van Andel 1995.
[35] E.g. Perlès 2001; Johnson/Perlès 2004.
[36] Weninger et al. 2009.
[37] Perlès 2001; Johnson/Perlès 2004.

Country	Site	Total ^{14}C-Dates	Table No.
Greece	Mandalo	19	Tab. 1
Greece	Sitagroi	24	Tab. 2
Greece	Dikili Tash	24	Tab. 3
Greece	Pevkakia	4	Tab. 4
Greece	Tharrounia	12	Tab. 5
Greece/Bulgaria (border)	Promachon	12	Tab. 6
Greece	Achilleion	44	Tab. 7
Greece	Nea Nikomedeia	16	Tab. 8
Bulgaria	Yunacite	25	Tab. 9
Bulgaria	Ezero	58	Tab. 10
Bulgaria	Drama-Merdžumekja	18	Tab. 11
Bulgaria	Varna	19	Tab. 12
Bulgaria	Azmak	34	Tab. 13
Bulgaria	Drama-Gerena	10	Tab. 14
Bulgaria	Kremenik	10	Tab. 15
Bulgaria	Karanovo	46	Tab. 16
Bulgaria	Čavdar	28	Tab. 17
Romania	Băile Herculane	5	Tab. 18
Romania	Cernavodă	3	Tab. 19
Romania	Drăguşeni	6	Tab. 20
Romania	Scânteia	8	Tab. 21
Romania	Pietrele	23	Tab. 22
Romania	Poduri	13	Tab. 23
Romania	Căscioarele	33	Tab. 24
Romania	Parţa	14	Tab. 25
Romania	Dudeştii Vechi	4	Tab. 26
	Culture		
Ukraine (North Pontic)	Cucuteni-Tripolye	97	Tab. 27
		Σ = 609	

*Table A. Overview of Radiocarbon Dates (Appendix **Tab. 1–27**)*

data to the site map of Gallis (**Fig. 5**),[38] it becomes clear that post-depositional erosion is an insufficient explanation for the large disparity in site quantities between the different periods (EN=112 MN=117, LN1=135, LN2=140, FN=34, and EBA=133). Of course, we must allow for a redistribution of preferred sites during the different periods as well as for differences in data quality. Nevertheless, the site counts clearly indicate that the lower (eastern) Thessalian plain was continuously and densely occupied by farming communities during all periods, with the exception of the FN. The existence of a major economic switch from the LN2 to the FN becomes all the more apparent, if we allow for the observation that FN sites in the upland regions of southeastern Thessaly have the highest density; from this it may be inferred that these sites were occupied mainly by pastoralists.[39] Interestingly, with the onset of the Early Bronze Age (ca. 3300 calBC) there is a switch back from pastoralism to floodplain-based farming.

Figure 6 provides an overview of the total available ^{14}C data for the Neolithic and Early Bronze Age of Greece (ca. 6200–3000 calBC). The heading of this figure includes the Thessalian cultural sequence as defined by Gallis.[40] We note, in particular, that the major cultural hiatus between the FN and the EBA (which separates the painted pottery of Rachmani style from the largely unpainted EBA-style pottery) also shows up in the general lack of ^{14}C data for the entire period (ca. 4000–3000 calBC). A further indication of a major gap in the Greek cultural sequence, which encompasses the entire period, is provided by stratigraphic observations and ^{14}C data from Mandalo and Sitagroi. At the site of Mandalo (western Macedonia), EBA pottery is found in direct stratigraphic superposition above the painted Rachmani pottery. The same stratigraphic superposition of EBA and FN, and again with a gap of 800–1000 cal years between the two periods, is also evident at the site of Sitagroi (eastern Macedonia). The ^{14}C data from Mandalo[41] show that the painted Rachmani-style pottery (i. e., the Greek FN) ends ca. 4100 calBC. The existence of a similar hiatus that separates the Greek FN from the Greek EBA by 800–1000 years is indicated by ^{14}C data from the central Macedonian site of Promachon.[42]

It is interesting to note that there is evidence that Thessaly was not entirely deserted by farming communities during the 4100–3300 calBC interval (**Fig. 6**). This is indicated by important cultural finds from the coastal (*sic* ! see above) site of Petromagula; notably, the presence of bowls or lids of the so-called "Bratislava" type. Similar finds (probably imported to Petromagula) are known from sites of the Boleráz/Cernavodă III cultures, which have a widespread distribution in eastern and southeastern Europe.[43] Further indications for settlement of the Thessalian coast dating to the second half of the 4th millennium calBC come from Mikrothives.[44]

[38] Gallis 1992.

[39] Perlès 2001; Johnson/Perlès 2004.
[40] Gallis 1992.
[41] Maniatis/Kromer 1990.
[42] Koukouli-Chryssanthaki 2007.
[43] Maran 1998.
[44] Adrymi-Sismani 2007.

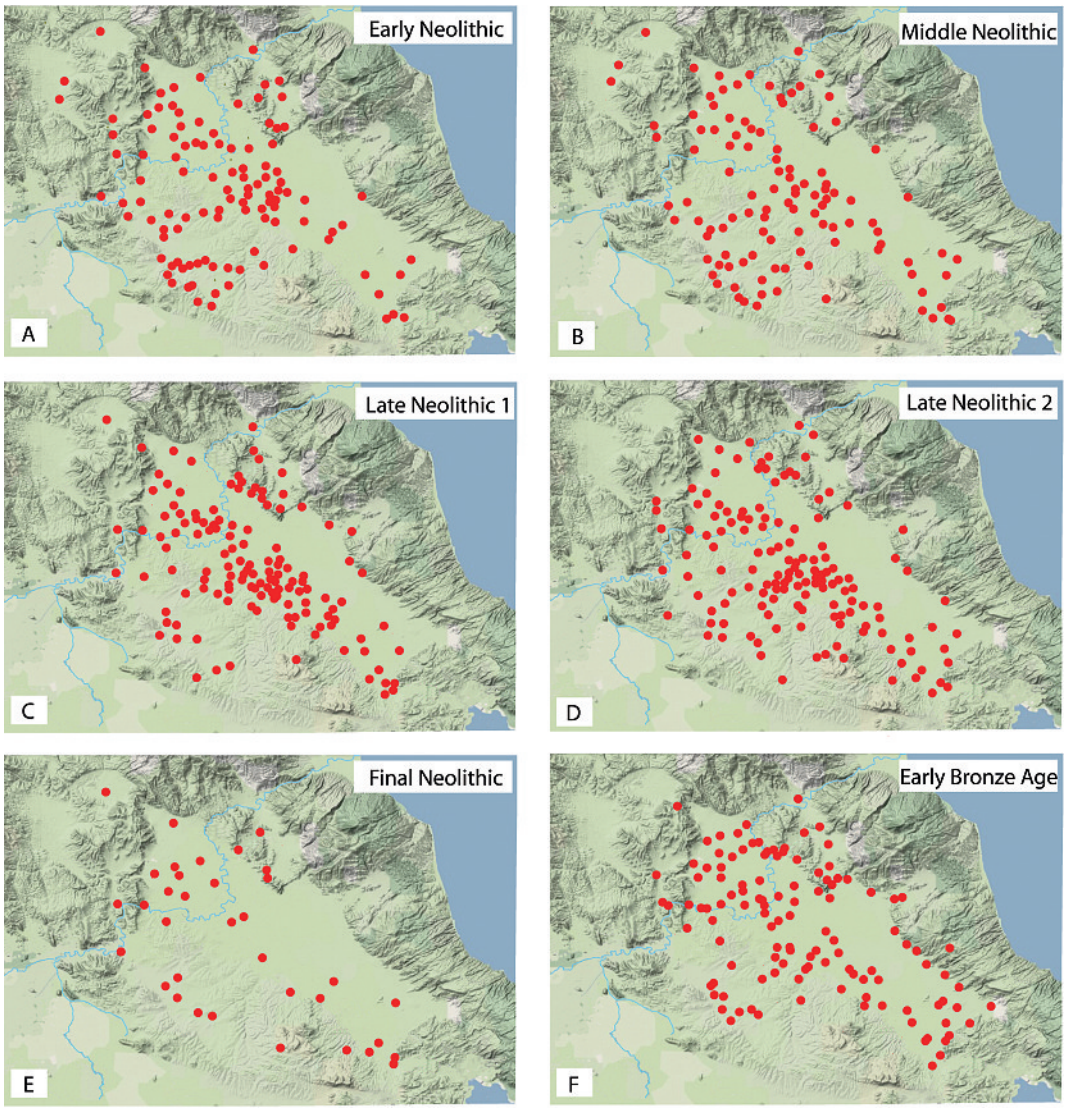

Fig. 5. Distribution of prehistoric settlements in Thessaly (Greece). From top to bottom: (A) Early Neolithic; (B) Middle Neolithic; (C) Late Neolithic 1; (D) Late Neolithic 2; (E) Final Neolithic; (F) Early Bronze Age. Sites georeferenced and projected onto SRTM imagery with Globalmapper® from Gallis (1992), Perlès (2001), Hanschmann (1976, Fig. 2), van Andel (unpubl., pers. comm).

Bulgaria

For Bulgaria the relative and absolute chronology of the prehistoric periods is comparatively well-established.[45] This is mainly due to the large number of deeply stratified Neolithic, Eneolithic and Bronze Age tell settlements that have been selectively ^{14}C dated by the Berlin Radiocarbon Laboratory.[46] From the distribution of ^{14}C ages (**Fig. 7**) it is apparent that there is a glaring gap in the Bulgarian ^{14}C sequence between 4100 and 3200 calBC just as in Greece. In Bulgarian terminology this time interval corresponds to the Transitional Period, which separates the Late Eneolithic from the Early Bronze Age.

The general paucity of archaeological data from the Transitional Period (henceforth, TP; 4100–3200 calBC) is well-known to Bulgarian researchers. Whereas in Greece there is an almost complete gap in the ^{14}C sequence, in Bulgaria there is at least one known site where the switch in economy during the TP is well-dated by radiocarbon: the cave site of Yagodina, located in the Rhodope Mountains (western Bulgaria). This site has supplied evidence in the form of hearths, pottery, animal bones and lithics for semi-permanent occupation during the Bulgarian TP.[47] Due to the site's location in a semi-mountainous area, it has been proposed that it was occupied seasonally by people who were chiefly pastoralists.[48] As can be taken from **Figure 7**, the site of Yagodina has supplied a small but consistent set of ^{14}C ages that can be assigned to the early 4th millennium calBC. Just as in Greece during the

[45] Gaul 1948; Todorova 1984; Todorova 1995; Pernicheva 1995; Boyadziev 1995.
[46] Quitta/Kohl 1969; Neustupny 1973; Todorova 1978; Görsdorf/Bojadžiev 1996.

[47] Аврамова 1991.
[48] Аврамова 1991.

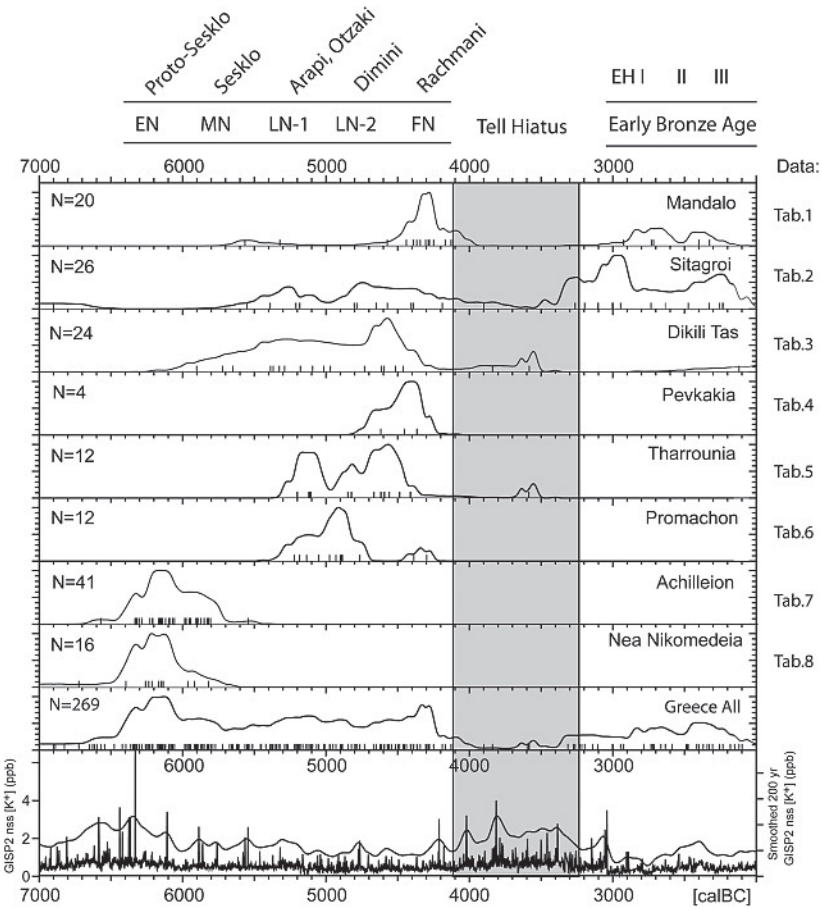

*Fig. 6. Above: Neolithic and Early Bronze Age radiocarbon data from selected northern and central Greek sites (Mandalo, Sitagroi, Dikili Tas, Pevkakia, Tharrounia, Promachon, Achilleion and Nea Nikomedeia). Below: Greenland GISP2 nss [K⁺] chemical series (both raw data and data with a 200-year Gaussian-smoothing filter) as a proxy for RCC conditions. The box indicates desertion of tell settlements during the RCC interval, ca. 4100–3200 calBC. See appendix for ^{14}C data tables (**Tab. 1–8**).*

time interval of 4100–3200 calBC, the Bulgarian TP is also characterised by a switch from an agrarian (tell-based) economy to a pastoral one, which, in the material record, is mainly manifested in the form of small ephemeral settlements in upland locations.

Before proceeding to our main topic, the study of potential RCC impact in Ukraine, we conclude our review of the situation in Greece, Bulgaria and Romania with the brief description of some new (exploratory) chronological results achieved for the Bulgarian multi-layer site Dipsis (Ezero). This is an addendum to our previous studies of ^{14}C ages from this site.[49] As demonstrated in **Figures 8; 9**, there exists the distinct possibility that the EBA settlement at Ezero was re-occupied following a long (~1000 yr) abandonment during the 4.2–3.0 ka calBC RCC interval, at the very time that climate conditions would probably have become attractive again for farming and animal husbandry. Whether the apparent gap in the pottery sequence between Ezero A (Level 6) and Ezero B (Level 5) – which is clearly indicated by pottery seriation – represents a true settlement gap, and also whether this gap is in any way related to RCC,[50] is impossible to conclude with the presently available data.

Romania

Due to ongoing large-scale archaeological research at the Romanian tell site of Pietrele/Romania,[51] an accurate date is now available for the end of the Copper Age in the Lower Danube region. Although the exact reasons for site abandonment at Pietrele are still subject of scientific enquiry, it is now clear that the settlement was finally abandoned following a major conflagration at 4250 ± 30 calBC.[52] Within error limits this date is directly equivalent to the end of the long-ranging Kodžadermen-Gumelniţa-Karanovo-VI (henceforth, KGK VI) cultural complex, which has a wide geographic distribution in Bulgaria and Romania.[53] In geographically broader terms, this date covers the end of the Chalcolithic period in Southeast Europe (**Fig. 10**). The unexpectedly old ^{14}C ages for Varna cemetery[54] in the Bulgarian Black Sea littoral require further studies.[55]

By mapping the KGK VI sites according to relative chronology, it becomes clear that *prior* to 4250 calBC the entire region of the Lower Danube and its tributaries was densely inhabited (**Fig. 11a**). Following the collapse of the KGK VI complex, in the following cultural period (**Fig. 11b**) all sites south of the Danube River had been deserted. North of the Danube, settlement densities remain high but are now of the monolayer type that is characteristic for the new Cernavodă I culture. The desertion of the KGK VI core region is especially evident for the previously densely populated river valley that connected large sites like Pietrele (in the northwest) with Varna and Sava (in the southeast). Interestingly, as opposed to the multilayered KGK VI tell sites, the settlements of the new Cernavodă I culture are single-phased (i. e. most likely short-lived). To conclude, in Romania (just as in Greece and Bulgaria) the end of the Copper Age is characterised by widespread abandonment of the centralised tell mode of economy, followed by a switch to a more ephemeral pastoralist economy. This switch appears on a supra-regional scale that encompasses practically all regions of Southeast Europe (Greece, Romania, Bulgaria) as well as northwestern Anatolia and the western coast of Turkey. It continues during the entire time interval of 4200–3200 calBC until – around

[49] Weninger 1992; Weninger 1995.

[50] Cf. captions to **Fig. 8** and **Fig. 9**.

[51] Hansen et al. 2007a–b.

[52] Weninger et al. 2010.

[53] Hiller 1989.

[54] Higham et al. 2007a–b.

[55] Krauß pers. comm. 2012; Nikolov pers. comm. 2012; Reingruber pers. comm. 2012.

3200 calBC – we see the beginnings of the Early Bronze Age, and many of the previous tell sites are re-occupied. In chronological terms, these cultural trajectories appear entirely synchronous with the RCC mechanism. Consequently, the hypothesis has been put forward that the economy in these regions had the property that it can switch (abruptly) on and off between two different economic modes. These are: (1) centralised tell-based farming; and (2) mobile pastoralism, depending on the prevailing environmental and societal impact of the "Little Ice Age" conditions during this time interval.[56]

Ukraine

In stark contrast to the other cases explored in this paper, the situation in Ukraine during the RCC interval, corresponding roughly with the relative chronological phases of Tripolye BI–BII, BII, CI and CI–II, was not one of settlement abandonment. In fact, in the region between the Southern Bug and Dnieper rivers, the "giant-settlement" or "megasite" phenomenon of the Western Tripolye culture (ca. 4150–3500/3400 calBC) was largely synchronous with this climate event. These settlements, which were of approximately 100–340 ha in area[57] and had populations upwards of several thousand individuals, were the largest population centres of the European Neolithic and Eneolithic. Eleven Western Tripolye sites, which have only been known to archaeologists for about forty years,[58] are categorized as giant-settlements among an accompanying body of small- and medium-sized settlements. During at least two periods of the giant-settlement phenomenon, dendritic-type local settlement systems (or K = 2, according to the Central Place Theory[59]) emerged,[60] and there has been much lively debate regarding the socio-political complexity of these settlements. To one extreme, they have even been labelled as "proto-cities".[61] In general, this assertion does not agree with the nature of the archaeological materials present, which do not show any large degree of social differentiation or the sort of continual occupation expected of urban formations.[62]

Discussion of the Cucuteni-Tripolye cultural complex vis-a-vis societal complexity should always be contextualized against the fact that the well-developed relative chronology dictates that settlements, giant- or otherwise, were single-occupation sites with a settlement period of approximately 50 to 80 years.[63] This also has important implications for discussion of the RCC mechanism; in Ukraine there is not the strict dichotomy of floodplain-farming communities versus mobile pastoralists, which is proposed for much of Southeast Europe. It is almost certain that the rapidly shifting settlement patterns, which are particularly dominant in the forest-steppe zone of Ukraine were the result of a regionally adapted form of economic practice, with the region constituting the "ideal environment for an agricultural and husbandry [-based] economic system".[64] The Cucuteni-Tripolye subsistence economy primarily took the form of dryland cereal cropping accompanied by cattle husbandry, although the contribution of horses, small ruminants and wild resources such as red deer and fish should not be underestimated. Given the broad and sparsely populated territories available for settlement in the forest-steppe zone, these communities were perhaps already more itinerant in nature and more flexible to changing climatic conditions. The longevity of the Eneolithic in Ukraine, which persisted until

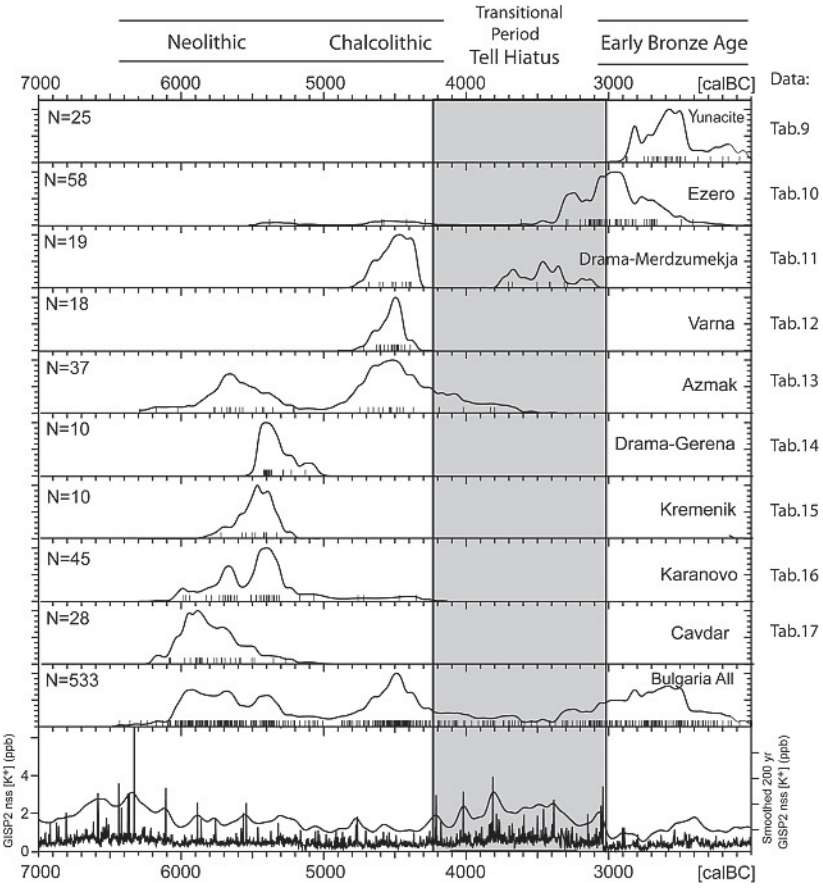

*Fig. 7. Neolithic and Early Bronze Age radiocarbon data from selected Bulgarian sites. Lower section – Greenland GISP2 nss [K^+] chemical series (both raw data and data with a 200-year Gaussian-smoothing filter) as a proxy for RCC conditions. The box indicates desertion of tell settlements during the RCC interval, ca. 4100–3200 calBC. See appendix for ^{14}C data tables (**Tab. 9–17**).*

[56] Weninger et al. 2009.
[57] Дяченко 2010a, 20–21.
[58] Шишкін 1973.
[59] Christaller 1966.
[60] Дяченко in press.
[61] Шмаглій/Відейко 1993; Videiko 2003; Videiko 2005.
[62] E.g. Массон 1990; Збенович 1990; Monah 2003; Anthony 2007.
[63] Рыжов 1990; Рыжов 1999; Рижов 2007; Kruts 2008a; Diachenko/Menotti 2012.
[64] Kruts 2008a, 45.

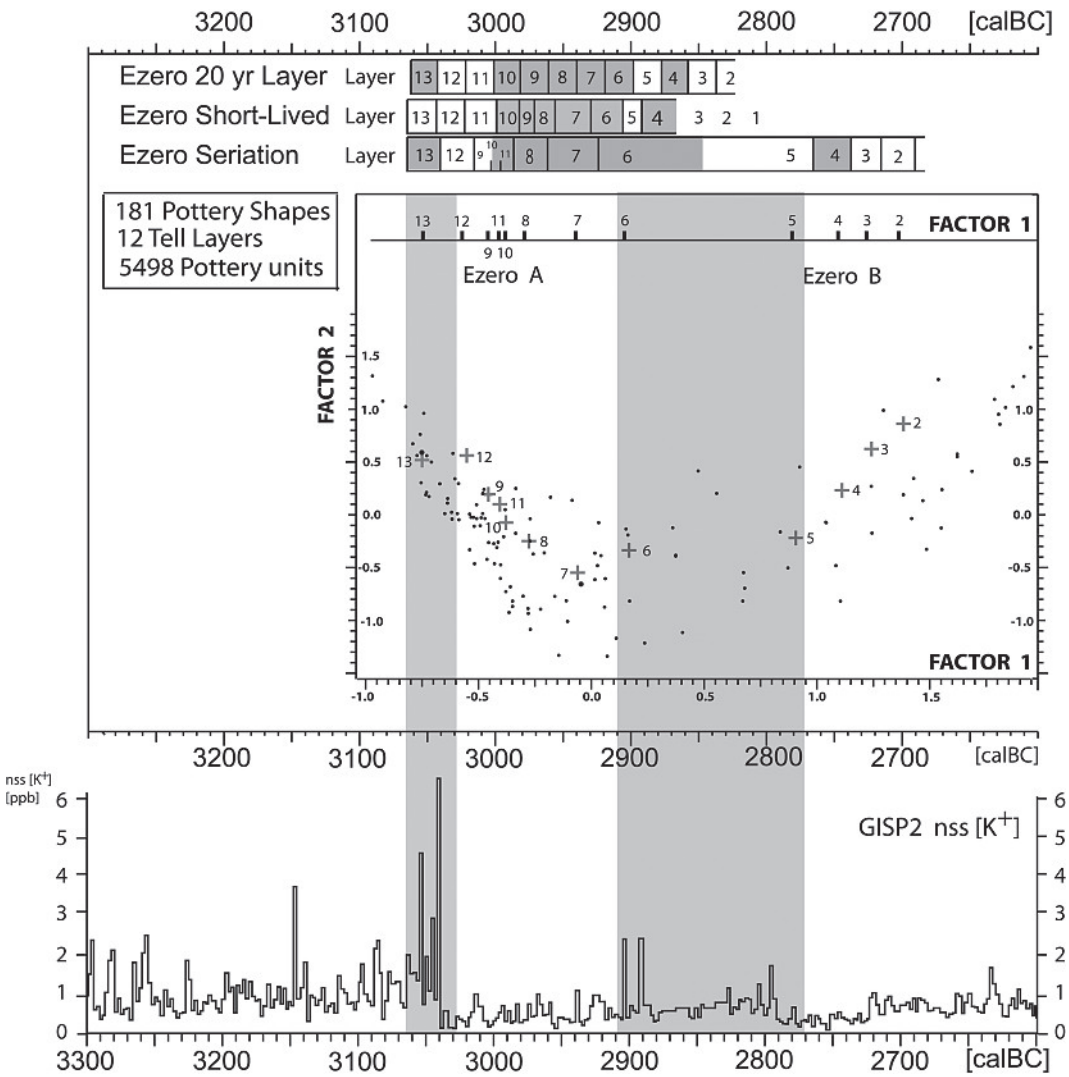

*Fig. 8. Stratified EBA ^{14}C ages from Ezero (Tell Dipsis) in comparison to Greenland GISP2 nss [K^{+}] chemical series, with an inset displaying pottery seriation by Correspondence Analysis (CA) scaled to ^{14}C wiggle-matching results achieved by assuming a linear relation between CA-Factor 1 and calendric time. For comparison purposes the graph also shows ^{14}C wiggle-matching results achieved by alternative methods. Upper section: Linear 20-year phase modelling and selection of short-lived samples. Shaded boxes indicate Ezero layers for which ^{14}C ages are available, depending on method. See appendix for ^{14}C data (**Tab. 10**). Interpretation: (1) Within error limits of a few decades, the earliest EBA level (level 13) at Ezero is settled at the end of the 6.2–6.0 ka calBP RCC interval; (2) there exists the possibility that the distinct gap in the CA seriation ca. 2900 calBC may be due to temporary site abandonment related to RCC. Note: according to archaeological reasoning the few calibrated ^{14}C ages taken from the upper levels at Ezero are anomalously old compared to ages derived from other Bulgarian EBA sites (pers. comm. V. Nikolov 2012).*

approximately 3000 calBC, makes it difficult to argue for a clear-cut climatically determined collapse on the same terms as proposed for settlement systems in Greece, Bulgaria and Romania. In fact, the transition to pastoralism, in the form of the Late Tripolye (CII phase) communities, occurs around the end of the RCC interval.

Analysis of ^{14}C data from the Cucuteni-Tripolye cultural complex is often confounded by the large amount of dates processed by the Kiev Radiocarbon Laboratory (lab code Ki), which are of variable quality and have been criticized on several occasions.[65] As an example, the Ki dates returned for the Tripolye A sites in the Dniester region are significantly older than the earliest Precucuteni dates in Romania. A similarly unfavourable situation can be seen in the dates belonging to later periods (Tripolye CI and CII), which tend to be much too late and lack the defined transitions between periods that are obvious in the archaeological material. In either situation, reliance on ^{14}C dates alone tends to lead

[65] Збенович 1989; Гаскевіч 2007, 138–141; Kruts 2008b, 232; Дяченко 2010b, 42–43.

to the false conclusion that the Cucuteni-Tripolye complex was synchronous with both Neolithic (e. g. Linearbandkeramik, Boian, and Criş) and Early Bronze Age (e. g. Yamnaya) cultures. In the former case this is utterly improbable, as these cultures formed the base for the development of the Precucuteni/Tripolye A culture (the two being synchronous and synonymous), which in turn was the base for the development of the first uniquely "Tripolian" material beginning from the end of phase BI onwards.[66] As for the latter case, one would expect to find some exchange of material between the late Tripolye and Early Bronze Age groups (one does not).

Ultimately, in order to come to an absolute chronology that is in approximate agreement with the archaeological material, the most simple solution is to liberally interpret (or exclude altogether) the dates from the Kiev lab, which has been done previously on several occasions.[67] The results of the periodisation presented here (**Tab. B; Tab. C**) should be viewed in an abstract sense, as a tool for application to discrete cultural periods in a diachronic model environment. We have constructed this periodisation with the aim of attaining calendric age intervals for the detailed site distribution maps published by Manzura.[68] This scheme disguises significant variation in cultural assemblages, including periodic synchronous distributions of settlements belonging to ostensibly different "periods"; for example, Diachenko and Menotti[69] suggest that BII and CI were synchronous for nearly a century in the Southern Bug-Dnieper interfluve. It should be stressed that the chief utility of the few available Cucuteni-Tripolye ^{14}C dates is their ability to contextualize the comparatively advanced relative dating of sites.

The current understanding of the Tripolye relative chronology is particularly well-developed, a system descended from the original periodisation laid out by T. S. Passek[70] and refined on several occasions over six decades.[71] As new and more reliable ^{14}C data become available, such as the recent Oxford dates from the Tripolye CI giant-settlement at Tal'yanki,[72] slight refinements may be made. Some measure of cynicism should be accompanied by the direct application of many of the Cucuteni-Tripolye absolute dates to a climatic model, as the often-times large disparity between relative and absolute chronologies serves to highlight the limitations of the latter. Generally speaking, any anomalies that might potentially be found should not be interpreted as gaps in the material sequences. The multi-group analysis presented here (**Fig. 12**) serves to illustrate the fairly smooth continuity of the Cucuteni-Tripolye complex as a whole. However, this continuity is misleading in some ways, as the broad categorization used here conceals a great deal of spatio-temporal variation. Studies of adaptive responses to climate in this context should always be made in reference to sub-regional and local relative chronologies in the form of local settlement group sequences, or even individual site data.

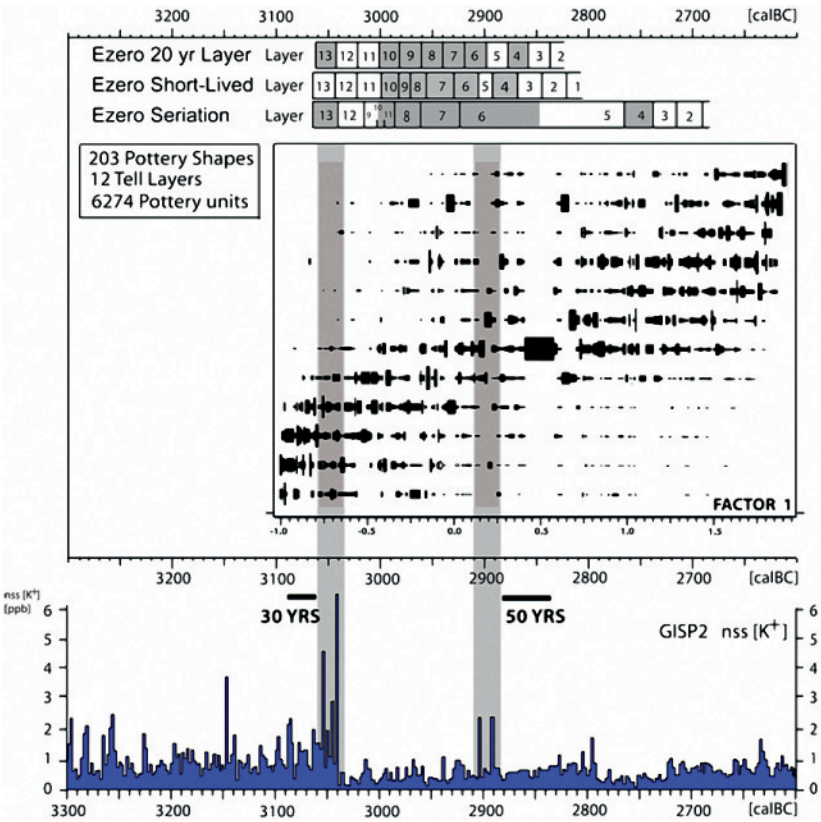

*Fig. 9. Data as shown in **Figure 8**, but with pottery seriation results shown as a battleship diagram, with pottery frequencies scaled to 100 % for individual settlement layers. With this representation it becomes clearer than in **Figure 7** that virtually no pottery finds are present in site deposits that have seriation dates between Level 6 and Level 5. Note: according to archaeological reasoning the few calibrated ^{14}C ages taken from the upper levels at Ezero are anomalously old compared to ages derived from other Bulgarian EBA sites (pers. comm. V. Nikolov 2012). Interpretation: within qualitatively estimated error limits (as indicated: 30/50 years) the site occupation: (1) begins at the end of the 6.2–6.0 ka calBP RCC-interval; and (2) appears to have been interrupted ca. 2900 calBC (i. e. synchronous with the corresponding GISP2 nss [K+] double-peak).*

Indications of Cucuteni-Tripolye climate change responses do in fact exist during the RCC interval. The most prominent among these is the migratory mechanism that prompted the Tripolye colonisations of the forest-steppe zone, which was previously related by A. V. Diachenko[73] to

[66] Цвек 2006.
[67] Telegin et al. 2003, 463–464; Дяченко 2010b, 41.
[68] Manzura 2005.
[69] Diachenko/Menotti 2012.
[70] Пассек 1949.
[71] Виноградова 1983; Рыжов 1999; Цвек 2006; Рижов 2007.
[72] Rassamakin/Menotti 2011, 651.
[73] Дяченко 2010b.

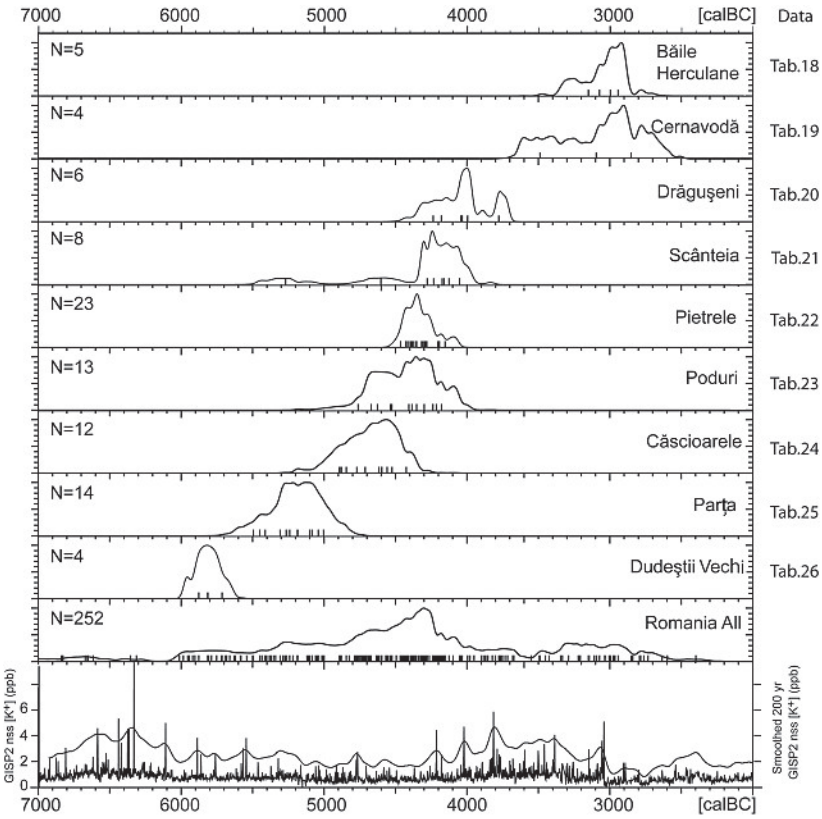

*Fig. 10. Neolithic and Early Bronze Age Radiocarbon Data from selected Romanian Sites (Baile Herculaneum, Cernavodă, Drăguşeni, Scânteia, Pietrele, Poduri Căscioarele, Parţa, Dudeştii Vechi). Below: Greenland GISP2 nss [K⁺] chemical series (both raw data and data with a 200-year Gaussian-smoothing filter) as a proxy for RCC conditions. The box indicates desertion of tell settlements during the RCC interval, ca. 4100–3200 calBC. See appendix for ^{14}C data tables (**Tab. 18–26**).*

episodes of aridity and cooling marked by eustatic change in the Black Sea. These were indicated in the palaeoclimatic scheme of V. A. Karpov,[74] and are among roughly twenty schemes focusing on Black Sea eustasy. Several authors have explored this topic in differing spatio-temporal contexts throughout Ukraine during the Holocene,[75] concluding these conditions would have had a great effect on the cultures of the Pontic steppe and nearby regions. Pertaining to the Cucuteni-Tripolye 'homeland' – that is, the Siret, Prut and Dniester river basins in Romania, Moldova and southwestern Ukraine – an increase in settlement density was accompanied by a degradation of the climate, prompting both the early (Cucuteni A/Tripolye BI) expansion into the forest-steppe, as well as the later (Tripolye BII to CI–II) migrations that led to the development of the giant-settlement phenomenon. It is unknown at this time how Black Sea eustasy relates to atmospheric RCC proxies; most likely it is in the same class of data as the oceanic component of RCC reinforced by episodes of glacial melt. It is proposed that statistical testing of RCC proxies against a model of Cucuteni-Tripolye demographic development, beyond verifying or rejecting correlations that are qualitatively suggested here, will bring a new perspective to regional climate studies, which subsequently may be compared against an extensive body of pre-existing research. Perhaps a syncretic account of many climate change schemes may contribute even more towards explaining variations in cultural adaptation.

Discussion

At present, based on results shown in **Figure 13**, we may postulate that RCC conditions influenced the movement of Cucuteni-Tripolye populations from the Siret-Prut and Prut-Dniester regions to the forest-steppe zone in Ukraine. Using the site distribution maps of Manzura[76] as first-order proxy for demographic development, in combi-

[74] First applied to archaeology in Бруяко 1989.

[75] E.g. Dolukhanov/Shilik 2007; Velichko et al. 2009.

[76] Manzura 2005.

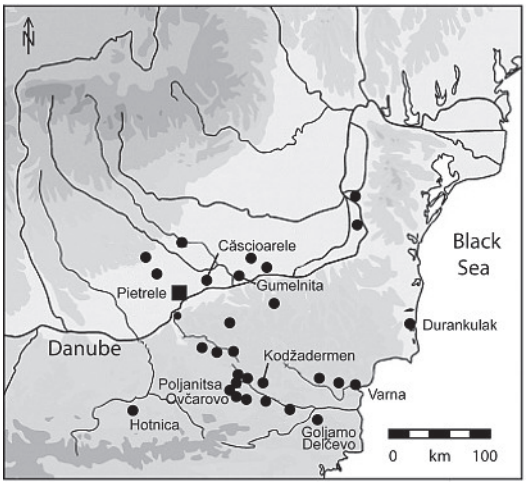

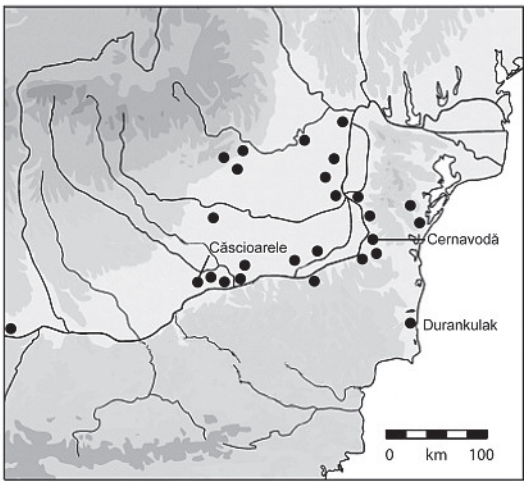

Fig. 11a (left). The Lower Danube region in the second half of the 5th millennium calBC. Dots: sites of the KGK VI complex (after Mayer 2008 map 8).

Fig. 11b (right). The Lower Danube region in the first half of the 4th millennium calBC. Dots: sites of the Cernavodă I culture (after Toderaş et al. 2009, plate 1,1)

nation with the calendric-scale time limits derived in **Table B**, we come to the following (basic) conclusions:

- the highest site density occurs prior to the onset of RCC conditions (map B: before ~4200 calBC);
- the Lower Danube is largely depopulated following the onset of RCC conditions (map C: ~ 4200–4000 calBC);
- following this, there is a major demographic expansion towards the northeast at the height of RCC conditions (maps C and D): ~4200–3600 calBC);
- finally, synchronous with the end of RCC conditions, the coastal regions of the Black Sea are colonised (map E: ~3600–3000 calBC).

While probably not so dramatic as the "explosive" demographic situation outlined by I. V. Manzura or V. G. Zbenovich as causation for the Western Tripolye migration events,[77] we may nonetheless obliquely make a similar point by advancing the hypothesis that a climatically determined change in regional resource potential constituted the root cause. We may find some common cause with G. L. Cowgill's assertion that migrations will often be provoked by a desire for "wealth increase" in individuals living along a high population density gradient.[78] Such a gradient certainly can be seen between the forest and forest-steppe zones at these times. The perceived economic benefit of exploiting a less-populated region is perhaps in itself adequate mo-

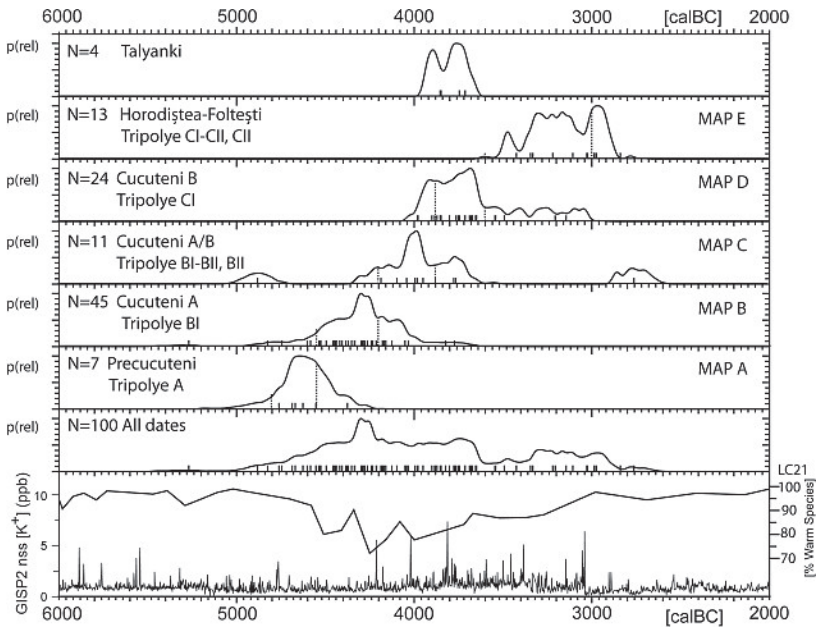

*Fig. 12. Cucuteni-Tripolye ^{14}C ages grouped by cultural phases (**Tab. C**) to achieve absolute age intervals for maps A–E (**Fig. 13**). Top section: ^{14}C ages shown independently for Talyanki. Below: Greenland GISP2 nss [K$^+$] chemical series (Mayewski et al. 1997) and Warm Species (%) from Marine Core LC21 as proxy for Sea Surface Temperature (Rohling et al. 2002). Time-intervals derived for maps A–E by additional data processing (**Tab. B**) are indicated by dashed lines. See appendix for ^{14}C data tables (**Tab. 27**).*

[77] Manzura 2005, 318 or Zbenovich 1996, 205.

[78] Cowgill 1975, 517.

Map (Fig. 13)	Corresponding cultural phases	N	μ	Σ	Adjusted for relative chronology	Statistical confidence
A	Precucuteni; Tripolye A	6	4641	82	ca. 4800–4550 calBC	~84 %
B	Cucuteni A; Tripolye BI	40	4304	139	ca. 4550–4200 calBC	~73 %
C	Cucuteni A/B; Tripolye BI–II and BII	9	3966	144	ca. 4200–3900 calBC	~63 %
D	Cucuteni B; Tripolye CI	22	3746	132	ca. 3900–3600 calBC	~74 %
E	Horodiştea-Folteşti; Tripolye CI–II and CII	13	3147	193	ca. 3600–3000 calBC	~77 %

*Table B. Determination of (partly schematic) Cucuteni-Tripolye chronological periods according to site distribution maps (**Fig. 13**) published by Manzura (2005). We have collated the corresponding ^{14}C ages from **Table 27**, with omission of obvious outliers, calculated the statistical confidence of the age ranges, and interpreted the confidence intervals to agree as closely as possible with considerations of relative chronology. This dating scheme diverges from others (cf. **Tab. C**), as it attempts to create discrete (i. e. non-overlapping) periods which may be applied in future demographic modelling (Harper, in press).*

Source	Tripolye A	Tripolye BI–II and BII	Tripolye CI	Tripolye CI–II	Tripolye CI
Diachenko (Дяченко 2010b)	4900/4800–4300/4200	4300/4200–3800	3800–3600	3600–3400	3400–2850
Rassamakin and Menotti (2011)	5100/5000–4400/4300	4400/4300–3900	3900–3450/3350	[not included]	3450/3350–3000/2900

Table C. Two recent periodisations proposed for Tripolye material, which seek to justify absolute and relative dating methods. The periodisation of Diachenko is additionally made in reference to Black Sea eustasy.

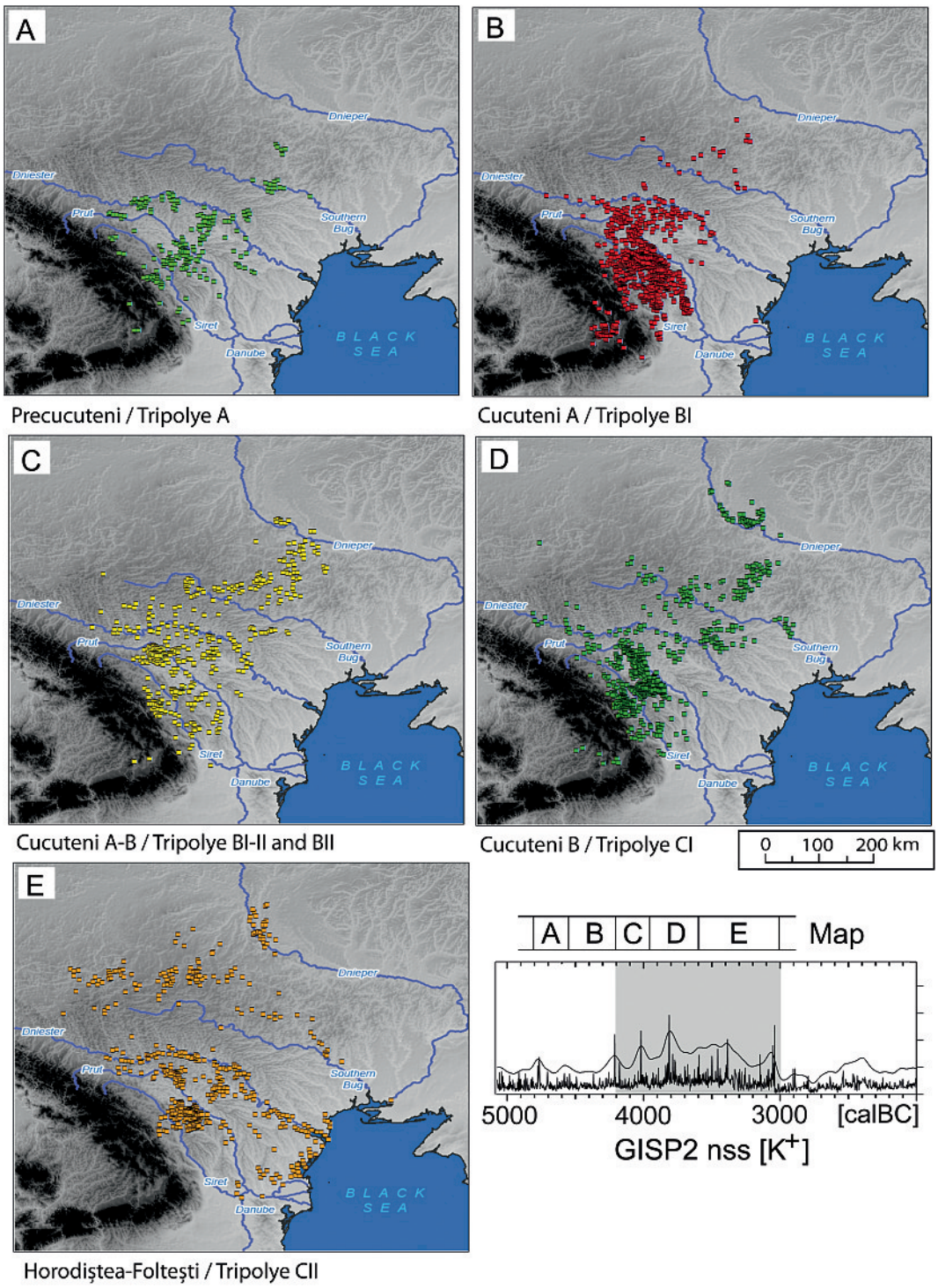

Fig. 13. Geographic distribution of archaeological sites in the Pontic region (~4800–3000 calBC) based on site mapping and cultural periodisation by I. V. Manzura (2005). Sites georeferenced and projected onto SRTM imagery with ArcGis®. The mapping corresponds to grouping of phases of the Cucuteni-Tripolye complex according to age limits given in ***Tab. B****. Lower right: Chronological relation between maps A–E and the GISP2 nss K^+ record as proxy for the strength of the Siberian High.*

tivation to migrate, even if conditions at the point of origin are not irredeemably grim. The presence of fortifications at settlements in the western territories but not in the Southern Bug-Dnieper interfluve (e. g. at the Western Tripolye giant-settlements) is also an interesting facet of this discussion. Ultimately, awaiting future research these points are open to broad speculation.

The overall picture of climate change in Ukraine is a very complicated one, and is likely confounded by seemingly contradictory forces occurring at varying scales according to different climatic proxies. A key aspect of D. W. Anthony's widely read work[79] is that climatic degradation in the Russian steppes beginning ca. 3300 BC brought pastoralist Early Bronze Age peoples to

[79] Anthony 2007.

Ukraine, who precipitated the Eneolithic collapse there by out-competing and/or absorbing the native populations. Perhaps the key distinction between Ukraine and the other geographic foci of this paper is that the climatically determined "sedentary versus pastoralist" scheme generally seems to work in reverse. Movement into the steppe is contraindicated during periods of poor climate, and the development of steppe-adapted late Tripolye groups, such as the Usatovo culture, is actually illustrative of wetter, more favourable conditions when the steppe was better-suited for ranging livestock. On a smaller scale, the migratory mechanism that formed the Tripolye giant-settlements, which are not at all a comparable phenomenon to the tell communities seen elsewhere, can be shown to support the idea of the RCC cooling mechanism as well as other climate studies.

Conclusions

With reference to pertinent palaeoclimatological, meteorological and archaeological literature, our detailed comparison of available ^{14}C data from Greece, Bulgaria, Romania and Ukraine during the Chalcolithic period suggests in many aspects a strong qualitative similarity with perceived trends in RCC proxy data. It is hoped that the discussion here may form a solid foundation for future investigations in climate archaeology, and at least incite greater general interest in palaeoclimatology as a means of understanding diachronic cultural variation. Far from a "catch all" scenario (i. e. an RCC "template" of expected behaviours), we suggest that human adaptive responses to climate change, although systematic, exhibit significant spatio-temporal variation.

Seemingly oppositional phenomena, such as giant-settlement formation in one region being synchronous with settlement abandonment in another, may very well have common causation. The degree to which the RCC mechanism has a role in this causation remains difficult to judge, although an initial effort at quantification has been made. Further research into our comparatively well-developed archaeological data sets for Ukraine has revealed a significant correlation between modelled demographic trends relating to the giant-settlement phenomenon and RCC proxies.[80] While these results are encouraging, we conclude that the success of future studies is contingent on the collation of more accurate and expansive regional archaeological and climatic data. These studies should not only examine super-regional climatic trends and the remote human responses on a local level, but multiple levels of intermediate responses in ancient environmental and social systems. In essence, we should strive to reconstruct the entire postulated causal chain. Particular emphasis should be placed on improving our conceptual modelling, via reference to historical and ethnographic analogies, of human vulnerability and adaptivity to climatic constraints.

[80] Harper 2013.

Acknowledgements

We are very thankful to Aleksandr Diachenko (Institute of Archaeology, National Academy of Sciences of Ukraine) as well as to Lee Clare (Institute of Prehistory, University of Cologne) for continual support and encouragement. Special thanks are due to Amit Tubi (University of Jerusalem, Israel) for invaluable information and sharing data (**Fig. 2**).

References

Adrymi-Sismani 2007
V. Adrymi-Sismani, Le site chalcolithique de Microthèbes au carrefour du monde égéen et des Balkans du Nord. In: I Galanaki/H. Tomas/Y. Galanakis/R. Laffineur (eds.), Between the Aegean and Baltic Seas. Prehistory across Borders. Proceedings of the International Conference "Bronze and Early Iron Age Interconnections and Contemporary Developments between the Aegean and the Regions of the Balkan Peninsula, Central and Northern Europe", University of Zagreb, 11–14 April 2005. Aegaeum 27, 2007, 73–79.

Anthony 2007
D. W. Anthony, The Horse, the Wheel, and Language: How Bronze-Age Riders from the Eurasian Steppes Shaped the Modern World (Princeton, Oxford 2007).

van Andel et al. 1990
T. H. van Andel/E. Zangger/A. Demitrack, Land use and soil erosion in prehistoric and historical Greece. Journal of Field Archaeology 17, 1990, 379–396.

van Andel et al. 1995
T. H. van Andel and C. N. Runnels, The earliest farmers in Europe. Antiquity 69, 1995, 481–500.

Biagi et al. 2005
P. Biagi/S. Shennan/M. Spataro, Rapid Rivers and Slow Seas? New Data for the Radiocarbon Chronology of the Balkan Peninsula. In: L. Nikolava/J. Fritz/J. Higgins (eds.), Prehistoric Archaeology and Anthropological Theory and Education. Reports of Prehistoric Research Projects 6–7 (Salt Lake City, Karlovo 2005) 41–50.

Boyadziev 1995
J. Boyadziev, Chronology of Prehistoric Cultures in Bulgaria. In: D. W. Bailey/I. Panayotov/S. Alexandrov (eds.), Prehistoric Bulgaria. Monographs in World Archaeology 22 (Madison 1995), 149–191.

Christaller 1966
W. Christaller, Central Places in Southern Germany (Englewood Cliffs, N. J. 1966).

Clare/Weninger 2010
L. Clare/B. Weninger, Social and Biophysical Vulnerability of Prehistoric Societies to Rapid Climate Change. Documenta Praehistorica 37, 2010, 283–292.

Clare et al. 2008
L. Clare/E. J. Rohling/B. Weninger/J. Hilpert, Warfare in Late Neolithic/Early Chalcolithic Pisidia, Southwestern Anatolia. Climate induced social unrest in the late 7th millennium calBC. Documenta Praehistorica 35, 2008, 65–92.

Clare 2013
L. Clare, Culture Change and Continuity in the Eastern Mediterranean and During Rapid Climate Change. Assessing the Vulnerability of Neolithic Communities to a Little Ice Age in the Seventh Millennium calBC. Unpublished doctoral thesis. University of Cologne (Köln 2013).

Cowgill 1975
G. L. Cowgill, On Causes and Consequences of Ancient and Modern Population Changes. American Anthropologist 77,3, 1975, 505–525.

Diachenko/Menotti 2012
A. V. Diachenko/F. Menotti, The gravity model: monitoring the formation and development of the Tripolye culture giant-settlements in Ukraine. Journal of Archaeological Science 39, 2012, 2810–2817.

Dolukhanov/Shilik 2007
P. M. Dolukhanov/K. K. Shilik, Environment, sea-level changes, and human migrations in the Northern Pontic area during late Pleistocene and Holocene times. In: V. Yanko-Hombach/A. S. Gilbert/N. Panin/P. Dolukhanov (eds.), The Black Sea Flood Question: Changes in Coastline, Climate and Human Settlement (Dordrecht 2007) 297–318.

Feurdean et al. 2008
A. Feurdean/S. Klotz/V. Misbrugger/B. Wohlfarth, Pollen-based quantitative reconstructions of Holocene climate variability in NW Romania. Palaeoclimatology, Palaeogeography, Palaeoecology 260, 2008, 494–504.

Fleitmann et al. 2008
D. Fleitmann/M. Mudelsee/S. J. Burns/R. S. Bradley/J. Kramers/A. Matter, Evidence for a widespread climatic anomaly at around 9.2 ka before present. Paleoceanography 23, 2008. PA1102, doi:10.1029/2007PA001519

Gallis 1992
K. I. Gallis, Atlas proīstorikon oikismon tis anatolikis Thessalikis pediadis (Larissa 1992).

Gallis 1994
K. I. Gallis, Results of Recent Excavations and Topographical Work in Neolithic Thessaly. La Thessalie. Quinze années de recherche archéologiques, 1975–1990. Actes Du Colloque International, Lyon, 17–22 Avril 1990. Volume A (Athènes 1994) 57–60.

Gaul 1949
J. H. Gaul, The Neolithic Period in Bulgaria. Bulletin of the American School of Prehistoric Research 16 (Cambridge, Massachusetts 1949).

GISP2 2012
Greenland Ice Sheet Project 2, Science Management Office, http://www.gisp2.sr.unh.edu/

Görsdorf/Bojadžiev 1996
J. Görsdorf/Y. Bojadžiev, Zur absoluten Chronologie der bulgarischen Urgeschichte. Berliner ^{14}C-Datierungen von bulgarischen archäologischen Fundplätzen. Eurasia Antiqua 2, 1996, 105–173.

Grootes et al. 1993
P. M. Grootes/M. Stuiver/J. W. C. White/S. Johnsen/J. Jouzel, Comparison of oxygen isotope records from the GISP2 and GRIP Greenland ice core. Nature 366, 1993, 552–554.

Hanschmann 1976
E. Hanschmann, Die Deutschen Ausgrabungen auf der Argissa-Magula in Thessalien III. Die Frühe und beginnende Mittlere Bronzezeit (Bonn 1976).

Hansen et al. 2007
S. Hansen/M. Toderaş/A. Reingruber/I. Gatsov/C. Georgescu/J. Görsdorf/T. Hoppe/P. Nedelcheva/M. Prange/J. Wahl/J. Wunderlich/P. Zidarov, Pietrele, Măgura Gorgana. Ergebnisse der Ausgrabungen im Sommer 2006. Eurasia Antiqua 13, 2007, 43–112.

Hansen et al. 2008
S. Hansen/M. Toderaş/A. Reingruber/I. Gatsov/F. Klimscha/P. Nedelcheva/R.. Neef/M. Prange/T. D. Price/J. Wahl/B. Weninger/H. Wrobel/J. Wunderlich/P. Zidarov, Der kupferzeitliche Siedlungshügel Măgura Gorgana bei Pietrele in der Walachei. Ergebnisse der Ausgrabungen im Sommer 2007. Eurasia Antiqua 14, 2008, 1–83.

Harper 2013
T. K. Harper, The effect of climatic variability on population dynamics of the Cucuteni-Tripolye cultural complex and the rise of the Western Tripolye giant-settlements. Chronika 3, 2013, 28–46.

Higham et al. 2007
T. F. G. Higham/C. Bronk Ramsey/F. Brock/D. Baker/P. Ditchfield, Radiocarbon dates from the Oxford AMS system: Archaeometry Datelist 32. Archaeometry 49, 2007, 1–60.

Higham et al. 2007
T. F. G. Higham/J. Chapman/V. Slavchev/B. Gaydarska/N. Honch/Y. Yordanov/B. Dimitrova, New perspectives on the Varna cemetery (Bulgaria) – AMS dates and social implications. Antiquity 81, 2007, 640–654.

Higham et al. 2008
T. Higham/J. Chapman/V. Slavchev/B. Gaydarska/N. Honch/Y. Yordanov/B. Dimitrova, New AMS Radiocarbon Dates for the Varna Eneolithic Cemetery, Bulgarian Black Sea Coast. Acta Musei Varnaensis VI, Studia in Memoriam Ivani Ivanov, The Varna Eneolithic Necropolis and Problems of Prehistory in Southeast Europe (Varna 2008) 95–112.

Hiller 1989
S. Hiller, Das Neolithikum in Karanovo und seine chronologische Stellung zu den gleichzeitigen Kulturen in Nordgriechenland und Serbien. In: Tell Karanovo und das Balkan-Neolithikum. Gesammelte Beiträge zum In-

ternationalen Kolloquium in Salzburg, 20. – 22. Oktober 1988 (Salzburg 1989) 165–179.

Johnson/Perlés 2004
M. Johnson/C. Perlès, An Overview of Neolithic Settlement Patterns in Eastern Thessaly. In: J. Cherry/C. Scarre/S. Shennan (eds.), Explaining social change: Studies in Honour of Colin Renfrew, McDonald Institute Monographs (Oxbow Books 2004) 65–79.

Kotsakis 1989
K. Kotsakis/A. Papanthimou-Papaefthimiou/A. Pilali-Papasteriou/T. Savopoulou/Y. Maniatis, /B. Kromer, Carbon-14 dates from Mandalo, W Macedonia. In: Y. Maniatis (ed.), Archaeometry, International symposium on archaeometry (Amsterdam, Elsevier 1989) 679–685.

Koukouli-Chryssanthaki 2007
Ch. Koukouli-Chryssanthaki/H. Todorova/I. Aslanis/I. Vajsov/M. Valla, Promachon-Topolnica. A Greek-Bulgarian archaeological project. In: H. Todorova/M. Stefanovich/G. Ivanov (eds.), The Struma/Strymon River Valley in Prehistory. Proceedings of the International Symposium, Strymon Praehistoricus. In the Steps of James Harvey Gaul 2 (Sofia 2007) 43–78.

Krauß 2010
R. Krauß, Zur Akkumulation von Prestigegütern im Westschwarzmeerraum während des 5. Jahrtausends v. Chr. In: C. Theune/F. Biermann/R. Struwe/H. Gerson (eds.), Zwischen Fjorden und Steppe. Festschrift für Johan Callmer zum 65. Geburtstag. Internationale Archäologie. Studia honoraria 31 (Rahden/Westf. 2010) 289–301.

Kruts 2008a
V. A. Kruts, Giant-settlements of the Tripolian Culture. In: A. G. Korvin-Piotrovskiy/F. Menotti (eds.), Tripolye Culture in Ukraine: the Giant-settlement of Talianki (Kiev 2008) 42–48.

Kruts 2008b
V. A. Kruts, The Relative and Absolute Chronology of the Tripolye Culture Settlements Between the Bug and Dnepr and in the Middle Podneprovye Region (Non-Calibrated Dates). In: A. G. Korvin-Piotrovskiy/F. Menotti (eds.), Tripolye Culture in Ukraine: the Giant-settlement of Talianki (Kiev 2008) 231–238.

Lang et al. 2010
B. Lang/A. Bedford/S. J. Brooks/R. T. Jones/N. Richardson/J. B. Birjs/J. D. Marshall, Early-Holocene temperature variability inferred from chironomod assemblages at Hawes Water, northwest England. The Holocene 20,6, 2010, 943–954.

László 1997
A. László, Datarea prin radiocarbon în arheologie (Bucureşti 1979.

Lazarovici 2010
C.-M. Lazarovici, New data regarding the chronology of the Precucuteni, Cucuteni and Horodiştea-Erbiceni cultures. In: J. Šuteková/P.Pavúk/P. Kalábhová/B. Kovar (eds.), Panta Rhei. Studies in Chronology and Cultural Development of South-Eastern and Central Europe in Early Prehistory presented to Juraj Pavúk on the Occasion of his 75th Birthday. Studia Archaeological et Mediaevalia XI (Bratislava 2010) 71–94.

Luca/Suciu 2012
S. A. Luca/C. Suciu, IPCTE Radiocabon Database. Romania and nearby areas from Neolithic to Eneolithic. 2006–2008. http://arheologie.ulbsibiu.ro/radiocarbon/download.htm

Maniatis/Kromer 1990
Y. Maniatis/B. Kromer, Radiocarbon Dating of the Neolithic Early Bronze Age Site of Mandalo, Western Macedonia. Radiocarbon 32,2, 1990, 149–153.

Mantu 2000
C. M. Mantu, Relative and absolute chronology of the Romanian Neolithic. Analele Banatului VII–VIII, 1999–2000, 75–105.

Manzura 2005
I. Manzua, Steps to the Steppe: or, how the North Pontic Region was Colonised. Oxford Journal of Archaeology 24,4, 2005, 313–338.

Maran 1998
J. Maran, Die Badener Kultur und der ägäisch-anatolische Bereich. Germania 76, 1998, 497–525.

Marino et al. 2009
G. Marino/E. J. Rohling/F. Sangiorgi/A. Hayes/J. L. Casford/A. F. Lotter/M. Kucera/H. Brinkhuis, Early and middle Holocene in the Aegean Sea: interplay between high and low latitude climate variability. Quaternary Science Reviews 28, 2009, 3246–3262.

Mayewski et al. 1997
P. A. Mayewski/L. D. Meeker/M. S. Twickler/S. Whitlow/Q. Yang/W. B. Lyons/M. Prentice, Major features and forcing of high- latitude northern hemisphere atmospheric circulation using a 110,000- year long glaciochemical series. Journal of Geophysical Research 102, 1997, 26345–26366.

Mayewski et al. 2002
P. A. Mayewski/F. White/L. Margulis, The Ice Chronicles. The Quest to Understand Global Climate Change (University Press of New England 2002).

Mayewski et al. 2004
P. A. Mayewski/E. E. Rohling/J. C. Stager/W. Karlen/K. A. Maascha/L. D. Meeker/E. A. Meyerson/F. Gasse/S. van Kreveld/K. Holmgrend/J. Lee-Thorph/G. Rosqvist/F. Racki/M. Staubwasser/R. R. Schneider/E. J. Steig, Holocene climate variability. Quaternary Research 62, 2004, 243–255.

Meeker/Mayewski 2002
L. D. Meeker/P. A. Mayewski, A 1400-year high-resolution record of atmospheric circulation over the North Atlantic and Asia. The Holocene 12,3, 2002, 257–266.

Meyer 2008
D. Meyer, Der westpontische Raum am Ende der frühen Kupferzeit (Langenweißbach 2008).

Monah 2003
D. Monah, A Ghost is Haunting Europe: the Neolithic Proto-cities. In: Tripolian Settlements-Giants: The International Symposium Materials (Kiev 2003) 239–243.

Neustupny 1973
E. E. Neustupny, Absolute Chronology of the Aeneolithic Period. In: M. Garašanin (ed.), Actes du VIIIe Congrès International des Sciences Préhistorique et Protohistorique 2 (Belgrade 1973) 243–248.

Olson et al. 2001
D. M. Olson/E. Dinerstein/E. D. Wikramanayake/N. D. Burgess/G. V. N. Powell/E. C. Underwood/J. A. D'Amico/I. Itoua/H. E. Strand/J. C. Morrison/C. J. Loucks/T. F. Allnutt/T. H. Ricketts/Y. Kura/J. F. Lamoreux/W. W. Wettengel/P. Hedao/K. R. Kassem, Terrestrial Ecoregions of the World: A New Map of Life on Earth. BioScience 51, 2001, 933–938.

Perlès 2001
C. Perlès, The Early Neolithic in Greece: the first Farming communities in Europe. Cambridge World Archaeology (Cambridge 2001).

Pernicheva 1995
L. Pernicheva, Prehistoric Cultures in the Middle Struma Valley: Neolithic and Eneolithic. In: D. W. Bailey/I. Panayotov/S. Alexandrov (eds.), Prehistoric Bulgaria. Monographs in World Archaeology 22 (Madison 1995) 99–140.

Pross et al. 2009
J. Pross/U. Kotthoff/U. C. Müller/O. Peyron/I. Dormoy/G. Schmiedl/S. Kalaitzides/A. M. Smith, Massive perturbation in terrestrial ecosystems of the Eastern Mediterranean region associated with the 8.2 ka climatic event. Geology 37,10, 2009, 887–890. doi: 10.1130/G25739A.1

Quitta/Kohl 1969
H. Quitta/G. Kohl, Neue Radiocarbondaten zum Neolithikum und zur frühen Bronzezeit Südosteuropas und der Sowjetunion. Zeitschrift für Archäologie 3, 1969, 223–255.

Rasmussen et al. 2006
S. O. Rasmussen/K. K. Andersen/A. M. Svensson/J. P. Steffensen/B. M. Vinther/H. B. Clausen/M.-L. Siggaard-Andersen/S. J. Johnsen/L. B. Larsen/N. D. Dahl-Jensen/M. Bigler/R. Röthlisberger/H. Fischer/K. Goto-Azuma/M. E. Hansson/U. Ruth, A new Greenland ice core chronology for the last glacial termination. Journal of Geophysical Research 111, 2006. doi: 10.1029/2005JD006079.

Rassamakin/Menotti 2011
Yu. Ya. Rassamakin/F. Menotti, Chronological Development of the Tripolye Culture Giant-settlement of Talianki (Ukraine): ^{14}C Dating vs. Pottery Typology. Radiocarbon 53,4, 2011, 645–657.

Reimer et al. 2009
P. J. Reimer/M. G. L. Baillie/E. Bard/A. Bayliss/J. W. Beck/P. G. Blackwell/C. Bronk Ramsey/C. E. Buck/G. S. Burr/R. L. Edwards/M. Friedrich/P. M. Grootes/T. P. Guilderson/I. Hajdas/T. J. Heaton/A. G. Hogg/K. A. Hughen/K. F. Kaiser/B. Kromer/F. G. McCormac/S. W. Manning/R. W. Reimer/A. A. Richards/J. R. Southon/S. Talamo/C. S. M. Turney/J. van der Plicht/C. E. Weyhenmeyer, IntCal09 and Marine09 radiocarbon age calibration curves, 0–50,000 years calBP. Radiocarbon 51, 2009, 1111–1150.

Rohling/Pälike 2005
E. J. Rohling/H. Pälike, Centennial-scale climate cooling with a sudden cold event around 8,200 years ago. Nature 434, 2005, 975–979.

Rohling et al. 2002
E. J. Rohling/P. A. Mayewski/R. H. Abu-Zied/J. S. L. Casford/A. Hayes, Holocene atmosphere-ocean interactions: records from Greenland and the Aegean Sea. Climate Dynamics 18, 2002, 587–593.

Rohling et al. 2009
E. J. Rohling/R. H. Abu-Zied/J. S. L. Casford/A. Hayes/B. A. A. Hoogakker, "The Marine Environment: Present and Past." In: J. Woodward (ed.) The Physical Geography of the Mediterranean (Oxford 2009) 33–68.

Saaroni et al. 1996
H. Saaroni/A. Bitan/P. Alpert/B. Ziv, "Continental polar outbreaks into the Levant and eastern Mediterranean." International Journal of Climatology 16,10, 1996, 1175–1191.

Sahsamanoglou et al. 1991
H. S. Sahsamanoglou/T. J. Makrogiannis/P. P. Kallimpoulos, Some aspects of the basic characteristics of the Siberian anticyclone, International Journal of Climatology 11, 1991, 827–839.

Svensson et al. 2006
A. Svensson/K. K. Andersen/M. Bigler/H. B. Clausen/D. Dahl-Jensen/S. M. Davies/S. J. Johnsen/R. Muscheler/S. O. Rasmussen/R. Röthlisberger/J. P. Steffensen/B. M. Vinther, The Greenland Ice Core Chronology 2005, 15–42 ka. Part 2: Comparison to other records Quaternary Science Reviews 25, Shackleton special issue 24, 2006.

Telegin et al. 2003
D. Ya. Telegin/M. Lillie/I. D. Potekhina/M. M. Kovaliukh, Settlement and economy in Neolithic Ukraine: a new chronology. Antiquity 77, 2003, 456–471.

Thomas/Gleser 2011
M. Thomas/R. Gleser, Zur Problematik von Schichtenfolge und Fundverteilung am Fuße einer Tellsiedlung: Der Südosthang von Drama-Medržumekja. In: Taphonomie. Sitzung der AG Neolithikum im Rahmen des WSVA, Nürnberg 26.5.–27.5.2010. Fokus Jungsteinzeit. Berichte der AG Neolithikum 3 (Kerpen, Loogh 2011) 107–126.

Toderaş et al. 2009
M. Toderaş/S. Hansen/A. Reingruber/J. Wunderlich, Pietrele-Măgura Gorgana: o aşezare eneolitică la Dunărea de Jos între 4500 şi 4250 î.e.n. Materiale şi Cercetări Arheologice 2009, 39–90.

Todorova 1978
H. Todorova, The Eneolithic Period in Bulgaria. British Archaeological Reports Supplementary Series 49 (Oxford 1978).

Todorova 1995
H. Todorova, The Neolithic, Eneolithic and Transitional Period in Bulgarian Prehistory. In: D. W. Bailey/I. Panayotov/S. Alexandrov (eds.), Prehistoric Bulgaria. Monographs in World Archaeology 22 (Madison 1995) 79–98.

Treuil 1992
R. Treuil, 1992. Dikili Tash: village préhistorique de Macédoine orientale (Athènes 1992).

Tubi/Dayan 2012
A. Tubi/U. Dayan, The Siberian High: teleconnections, extremes and association with the Icelandic Low. International Journal of Climatology 33,6, 2012, 1357–1366. http://doi.wiley.com/10.1002/joc.3517

Velichko et al. 2009
A. A. Velichko/E. I. Kurenkova/P. M. Dolukhanov, Human socio-economic adaptation to environment in Late Paleolithic, Mesolithic and Neolithic Eastern Europe. Quaternary International 203, 2009, 1–9.

Videiko 2003
M. Yu. Videiko, Processes of Urbanization in Old Europe and Trypillia Culture Proto-Cities. In: Tripolian Settlements-Giants: The International Symposium Materials (Kiev 2003) 256–261.

Videiko 2005
M. Yu. Videiko, Looking for Tripillia Culture Proto-Cities. Self-published.

Vinther et al. 2006
B. M. Vinther/H. B. Clausen/S. J. Johnsen/S. O. Rasmussen/K. K. Andersen/S. L. Buchardt/D. Dahl-Jensen/I. K. Seierstad/M.-L. Siggaard-Andersen/J. P. Steffensen/A. M. Svensson/J. Olsen/J. Heinemeier, A synchronized dating of three Greenland ice cores throughout the Holocene. Journal of Geophysical Research 111,D13, 2006. doi: 10.1029/2005JD006921

Weisshaar 1989
H.-J. Weisshaar, Die deutschen Ausgrabungen auf der Pefkakia-Magoula in Thessalien I. Das späte Neolithikum und das Chalkolithikum. Beiträge zur ur- und frühgeschichtlichen Archäologie des Mittelmeerraumes 28 (Bonn 1989).

Weninger 1986
B. Weninger, High-precision calibration of archaeological radiocarbon dates. Acta Interdisciplinaria Archaeologia IV, 1986, 11–53.

Weninger 1992
B. Weninger, Fallstudien zur ^{14}C-Chronologie des Neolithikums in Bulgarien. Studia Praehistorica 11–12, 1992, 407–422.

Weninger 1995
B. Weninger, Stratified ^{14}C Dates and Ceramic Chronologies. Case Studies for the Early Bronze Age at Troy (Turkey) and Ezero (Bulgaria). Radiocarbon 37,2, 1995, 443–456.

Weninger et al. 2006
B. Weninger/E. Alram-Stern/E. Bauer/L. Clare/U. Danzeglocke/O. Jöris/C. Kubatzki/G. Rollefson/H. Todorova/T. van Andel, Climate Forcing due to the 8200 calBP event observed at Early Neolithic sites in the Eastern Mediterranean. Quaternary Research 66, 2006, 401–420.

Weninger et al. 2009
B. Weninger/L. Clare/E. Rohling/O. Bar-Yosef/U. Böhner/M. Budja/M. Bundschuh/A. Feurdean/H.-G. Gebel/O. Jöris/J. Linstädter/P. Mayewski/T. Mühlenbruch/A. Reingruber/G. Rollefson/D. Schyle/L. Thissen/H. Todorova/C. Zielhofer, The Impact of Rapid Climate Change on Prehistoric Societies during the Holocene in the Eastern Mediterranean. Documenta Praehistorica 36, 2009, 7–59.

Weninger et al. 2010
B. Weninger/A. Reingruber/S. Hansen, Konstruktion eines stratigraphischen Altersmodells für die Radiocarbondaten aus Pietrele, Rumänien. In: J. Šuteková/P. Pavúk/P. Kalábková/B. Kovár (eds.), PANTA RHEI. Studies on the Chronology and Cultural Development of the South-Eastern and Central Europe in Earlier Prehistory Presented to Juraj Pavúk on the Occasion of his 75th Birthday. Studia Archaeologica et Mediaevalia XI (Bratislava 2010) 35–58.

Weninger et al. 2011
B. Weninger/K. Edinborough/L. Clare/O. Jöris, Concepts of Probability in Radiocarbon Analysis. Documenta Praehistorica 38, 2011, 1–20.

Weninger/Clare 2011
B. Weninger/L. Clare, Holocene Rapid Climate Change in the Eastern Mediterranean: An Emerging Archaeological Climate Research Project. In: R. Krauß (ed.), Beginnings – New Research in the Appearance of the Neolithic between Northwest Anatolia and the Carpathian Basin: Papers of the International Workshop 8th–9th April 2009, Istanbul. Menschen-Kulturen-Traditionen. Studien aus den Forschungsclustern des Deutschen Archäologischen Instituts 1 (Rahden/Westf. 2011) 11–22.

Weninger/Jöris 2008
B. Weninger/O. Jöris, A ^{14}C age calibration curve for the last 60 ka: the Greenland-Hulu U/Th timescale and its impact on understanding the Middle to Upper Paleolithic transition in Western Eurasia. Journal of Human Evolution 55, 2008, 772–781.

WetterOnline 2012. Video downloaded on 28. Nov. 2012 from: http://video.wetteronline.de/?t=20120131jv&h=Schwarzmeertief-und-Bora

Yu et al. 2010
S.-Y. Yu/S. M. Colman/T. V. Lowell/G. A. Milne/T. G. Fisher/A. Breckenridge/M. Boyd/J. T. Teller, Freshwater Outburst from Lake Superior as a Trigger for the Cold Event 9300 Years Ago. Science 328, 2010, 1262–1266.

Zbenovich 1996
V. G. Zbenovich, The Tripolye Culture: Centenary of Research. Journal of World Prehistory 10,2, 1996, 199–241.

Аврамова 1991
М. Аврамова, Централните Родопи и проблемът за Преходния период от енеолита към бронзовата епоха. Археология 1991, 2, 51.

Бруяко 1989
И. В. Бруяко, Изменения литорали Северо-Западного Причерноморья с XX тыс. до н.э. (палеографические карты) In: Комплексные методы исследования археологических источников. Матер. к конф. 21–23 ноября 1989 (Москва 1989) 6–8.

Виноградова 1983
Н. М. Виноградова, Племена Днестровско-прутского междуречья в период растсвета трипольскои культуры (Кишинев 1983).

Гаскевіч 2007
Д. Гаскевіч, Синхронізація Буго-дністровського неоліту і неоліту Східної Европи. Проблема радіобуглецевіх дат. In: L. Bakalarska (ed.), Wspólnota dziedzictwa archeologicznego ziem Ukrainy i Polski. Krajowy ośrodek badań i dockumentaji zabytków (Warszawa 2007) 115–147.

Дяченко 2010a
О. В. Дяченко, До проблеми систематизації поселень західнотрипільської культури у межиріччі південного Бугу та Дніпра. Археологія і давня історія України 2010,2, 17–22.

Дяченко 2010b
А. В. Дяченко, Эвстатические колебания уровня Черного моря и динамика развития населения кукутень-трипольской общности. Stratum Plus 2010,2, 37–48.

Дяченко in press
О. В. Дяченко, Ієрархічні поселенські системи та проблема археологічних добірок. Analecta Archaeologica Ressoviensia, in press.

Збенович 1989
В. Г. Збенович, Поселение Бернашевка на Днестре. Наукова Думка (Киев 1989).

Збенович 1990
В. Г. Збенович, К проблеме крупных трипольских поселений. In: Раннеземледельческие поселения-гиганты трипольской культуры на Украине (Киев 1990) 10–12.

Массон 1990
В. М. Массон, Трипольское общество и его социально-экономические характеристики. In: Раннеземледельческие поселения-гиганты трипольской культуры на Украине (Киев 1990) 8–10.

Пассек 1949
Т. С. Пассек, Периодизация трипольских поселений (иии-ии тысячелетие до н. э). Материалы и исследования по археологии СССР No. 10, (Москва-Ленинград 1949).

Рыжов 1990
С. Н. Рыжов, Микрохронология трипольского поселения у с. Тальянки. In: Раннеземледельческие поселения-гиганты трипольской культуры на Украине (Киев 1990) 83–90.

Рижов 1999
С. М. Рижов, Кераміка поселень трипільської культури Буго-Дніпровського межиріччя як історичне джерело. Автореф. дисс. канд. іст. наук (Київ 1999).

Рижов 2007
С. М. Рижов, Сучасній стан вивчення культурно-історичної спільності Кукутень-Трипілля на теріторії України. In: О. Ольжич. Археологія (Київ 2007) 437–477.

Цвек 2006
Е. В. Цвек, Поселення східнотрипільської культури (короткій нарис) (Київ 2006).

Шишкін 1973
К. В. Шишкін. З практікі дешіфрування аерофотознімків у археологічніх цілях. Археологія 10, 1973, 32–41.

Шмаглій/Відейко 1993
М. М. Шмаглій/М. Ю. Відейко, Трипільські протоміста. Археологія 1993,3, 52–63.

Radiocarbon Data: Tab.1 Mandalo (40,86°N, 22,21 °E) Source: Kotsakis 1989

Lab-Code	14C-Age [BP]	δ13C [‰ PDB]	Material	Period	Phase	Locus
HD-9146	3860 ± 70	-25,20	charcoal	Bronze Age	--	Locus 1024
HD-9216	4130 ± 70	-25,70	charcoal	Bronze Age	--	Locus 7140
HD-9265	5540 ± 70	-24,10	charcoal	Neolithic	Phase Ib	Locus 4020
HD-9557	5440 ± 60	-25,30	charcoal	Neolithic	Phase Ib	Locus 5032
HD-9559	5490 ± 60	-24,70	charcoal	Neolithic	Phase II	Locus 2156
HD-9562	5600 ± 70	-25,80	charcoal	Neolithic	Phase Ib	Locus 3120
HD-9563	5430 ± 70	-24,00	charcoal	Neolithic	Phase II	Locus 2202a
HD-9595	6410 ±190	-24,70	charcoal	Neolithic	Phase II	Locus 2224
HD-9596	5290 ± 70	-24,80	charcoal	Neolithic	Phase II	Locus 7229
HD-9601	5710 ±150	-22,00	charcoal	Neolithic	Phase Ib	Locus 4007
HD-9602	5460 ±100	-25,20	charcoal	Neolithic	Phase II	Locus 1022
HD-9603	5520 ± 80	-24,80	charcoal	Neolithic	Phase Ib	Locus 3040
HD-9832	5420 ± 40	-24,50	charcoal	Neolithic	Phase II	Locus 7251
HD-9833	5460 ± 50	-24,80	charcoal	Neolithic	Phase II	Locus 7253
HD-9834	5340 ±100	-25,90	charcoal	Neolithic	Phase II	Locus 7275
HD-9835	4300 ±100	-26,00	charcoal	Bronze Age	--	Locus 8152
HD-9907	3920 ± 40	-25,10	charcoal	Bronze Age	--	Locus 8199
HD-9915	4130 ± 40	-25,30	charcoal	Bronze Age	Phase III	Locus 8231
HD-9939	5430 ± 45	-24,30	charcoal	Neolithic	Phase II	Locus 2292

Radiocarbon Data: Tab.2 Sitagroi (41,07 °N, 24,05 °E)

Lab-Code	14C-Age [BP]	δ13C [‰ PDB]	Material	Period	Phase		Locus
Bln-774	5100 ± 120	nd	charcoal	Neolithic	--	--	
Bln-778	6425 ± 100	nd	charcoal	Neolithic	--		ZA 70I
Bln-779	6625 ± 170	nd	charcoal	Neolithic	--		ZA 67
Bln-780	3870 ± 100	nd	charcoal	Bronze Age	EH II	--	
Bln-781	4085 ± 150	nd	organic	Bronze Age	EH II	--	
Bln-782	4310 ± 100	nd	charcoal	Bronze Age	EH II	--	
Bln-876	3965 ± 100	nd	charcoal	Bronze Age	EH II	--	
Bln-877	4170 ± 100	nd	charcoal	Bronze Age	EH II	--	
Bln-878	4395 ± 100	nd	charcoal	Bronze Age	EH II	--	
Bln-879	4550 ± 100	nd	charcoal	Bronze Age	EH II	--	
Bln-880	4510 ± 100	nd	charcoal	Bronze Age	EH II	--	
Bln-881	5555 ± 100	nd	charcoal	Neolithic	--	--	
Bln-882	5795 ± 100	nd	charcoal	Neolithic	--	--	
Bln-883	5545 ± 100	nd	seeds	Neolithic	--	--	
Bln-884	6240 ± 100	nd	charcoal	Neolithic	--	--	
Bln-885	7980 ± 150	nd	charcoal	Neolithic	--		ZA 63
BM-648	6265 ± 75	nd	charcoal	Neolithic	--		umulus niv. 2A67
BM-649	5904 ± 66	nd	charcoal	Neolithic	--	--	
BM-650a	4363 ± 56	nd	charcoal	Bronze Age	EH II	--	
BM-650b	5367 ± 85	nd	charcoal	Neolithic	--	--	
BM-651	4332 ± 79	nd	acorns	Bronze Age	EH II	--	
BM-652	3803 ± 59	nd	charcoal	Bronze Age	EH II		posthole
BM-653	3790 ± 78	nd	organic	Bronze Age	EH II	--	

Radiocarbon Data: Tab.3 Dikili Tash(41,05 °N, 24,15 °E) Source: Treuil, 1992

Lab-Code	14C-Age [BP]	δ13C [‰ PDB]	Material	Period	Phase		Locus
Ly-10089	4805 ± 40	--	bone	Neolithic	--	--	89/310 104/10/19
Ly-10090	5740 ± 45	--	bone	Neolithic	--	--	93/313 102/30/2
GIF-1426	6800 ± 150	--	--	Neolithic	Dikili Tas I	--	W30 (sond. est)
GIF-1735	6170 ± 160	--	--	Neolithic	Dikili Tas I	--	X29, fosse
GIF-1737	6400 ± 160	--	--	Neolithic	Dikili Tas I	--	X29
GIF-1739	2830 ± 110	--	--	Neolithic	Dikili Tas I	--	X30
GIF-1740	6450 ± 160	--	--	Neolithic	Dikili Tas I	--	X30
GIF-2627	6370 ± 170	--	--	Neolithic	Dikili Tas I	--	AA 28
GIF-2628	7020 ± 170	--	--	Neolithic	Dikili Tas I	--	AA 28
GIF-2629	6250 ± 160	--	--	Neolithic	Dikili Tas I	--	AA 28
GIF-2630	6720 ± 160	--	--	Neolithic	Dikili Tas I	--	W30 (sond. est)
GIF-1423	5650 ± 140	--	--	Neolithic	Dikili Tas II	--	W30
GIF-1424	5750 ± 140	--	--	Neolithic	Dikili Tas II	--	X29
GIF-1425	5750 ± 140	--	--	Neolithic	Dikili Tas II	--	R24
GIF-1736	5850 ± 160	--	--	Neolithic	Dikili Tas II	--	X29
GIF-1738	5600 ± 150	--	--	Neolithic	Dikili Tas II	--	R24
Ly-1062	6100 ± 200	--	--	Neolithic	Dikili Tas II	--	T24
Ly-1064	6040 ± 120	--	--	Neolithic	Dikili Tas II	--	U24
Ly-1061	6480 ± 270	--	--	Neolithic	Dikili Tas IIIA	--	T24
Ly-1602	3700 ± 230	--	--	Bronze Age	Dikili Tas IIIA	EH I	T24
Ly-1304	2370 ± 230	--	--	Bronze Age	Dikili Tas IIIB	EH I	Q24/25
Ly-1305	5030 ± 160	--	--	Bronze Age	Dikili Tas IIIB	EH I	P24
Ly-1063	3430 ± 120	--	--	Bronze Age	Dikili Tas IV	LH	Q25
Ly-1306	2870 ± 370	--	--	Bronze Age	Dikili Tas IV	LH	Q25/26

Radiocarbon Data: Tab.4 Pevkakia (39,29 °N, 22,90 °E) Source: Weisshaar 1989

Lab-Code	14C-Age [BP]	δ13C [‰ PDB]	Material	Period	Locus
Pta-1405	5630 ± 50	--	charcoal	Neolithic	Unteres Stratum
Pta-435	5770 ± 70	--	charcoal	Neolithic	Oberes Stratum
Pta-436	5520 ± 80	--	bone	Neolithic	Oberes Stratum
Pta-465	5510 ± 65	--	charcoal	Neolithic	Mittleres Stratum

Radiocarbon Data: Tab.5 Tharrounia (38,51 °N, 23,97 °E) Source: Sampson 1993

Lab-Code	14C-Age [BP]	Material	Period	Locus
DEM-170-136	6162 ± 36	charcoal	Neolithic	G28
DEM-171-137	6246 ± 49	charcoal	Neolithic	G30
DEM-172-138	5817 ± 37	charcoal	Neolithic	A4-5 T8
DEM-173-143	5737 ± 39	charcoal	Neolithic	G24 T5,6
DEM-174-144	5936 ± 69	charcoal	Neolithic	G14 T2
DEM-175-145	5961 ± 40	charcoal	Neolithic	A16 T1
DEM-91-113	5705 ± 64	charcoal	Neolithic	A21
DEM-92-103	5768 ± 89	charcoal	Neolithic	A21
DEM-93-104	4811 ± 42	charcoal	Neolithic	A6 T4
DEM-94-105	6150 ± 43	charcoal	Neolithic	A5 T7
DEM-95-106	5564 ± 276	charcoal	Neolithic	A13 T3
DEM-96-107	5657 ± 54	charcoal	Neolithic	A15

Radiocarbon Data: Tab.6 Promachon (41,36 °N, 23,55 °E) Source: Koukouli-Chryssanthaki 2007

Lab-Code	14C-Age [BP]	δ13C [‰ PDB]	Material	Period	Phase	Locus	Depth
Bln-3348	6000 ± 80	--	charcoal	Neolithic	Phase II	Hor.2b, Square M14,	0,90 m
Bln-3349	6240 ± 90	--	charcoal	Neolithic	Phase I	Hor.2c, Square O12,	1,20 m
Bln-3381	6270 ± 60	--	charcoal	Neolithic	Phase I	Hor.2b, Square J11,	0,80 m
Bln-3382	6100 ± 60	--	charcoal	Neolithic	Phase I	Hor.2c, Square J14,	1,10 m
DEM-1173	5996 ± 25	-25,00	charcoal	Neolithic	Phase II	Square ∑T, pasa 10,	79,30 m
DEM-1185	5895 ± 33	-25,00	charcoal	Neolithic	Phase II	Square ∑T, pasa 10,	79,31 m
DEM-1250	6068 ± 40	-25,00	charcoal	Neolithic	Phase II	Square ∑T, pasa 11,	78,99 m
DEM-1254	6038 ± 40	-25,77	charcoal	Neolithic	Phase II	Square ∑T,pasa 11,	78,99 m
HD-20457	6188 ± 38	--	charcoal	Neolithic	phase I	Square Γ,	78,17 m
HD-20459	5999 ± 47	-19,30	bone	Neolithic	phase III	Square ∑	
HD-20461	5447 ± 42	-19,00	bone	Neolithic	Phase III (IV)	Square IA,	80.05 m
HD-20462	5530 ± 48	-19,00	bone	Neolithic	Phase III (IV)	Square IA,	80.01 m

Radiocarbon Data: Tab.7 Achilleion (39,25° N, 22,42° E)

Lab-Code	14C-Age [BP]	δ13C [‰ PDB]	Material	Period	Phase	Locus
GrN-7435	7110 ± 70	--	charcoal	Neolithic	Phase IIIb	A-1-16
GrN-7434	7060 ± 70	--	charcoal	Neolithic	Phase IIIb	A-2-14
GrN-7432	7050 ± 100	--	charcoal	Neolithic	Phase IVa	D-4-2
GrN-7433	7025 ± 50	--	charcoal	Neolithic	Phase IVa	B-4-18 pit
GrN-7436	7295 ± 70	--	charcoal	Neolithic	Phase IIa	A-1-21
GrN-7437	7440 ± 55	--	charcoal	Neolithic	--	
GrN-7438	7390 ± 45	--	--	Neolithic	Phase Ib	C-1-21 Graben, locus 24/190-200
LJ-2940	6590 ± 80	--	charcoal	Neolithic	Phase IIIc	Sq B, Level 10
LJ-2941	6930 ± 60	--	charcoal	Neolithic	Phase IIIa1	Sq B, Quad 4, Level 15,17,18
LJ-2942	7200 ± 50	--	charcoal	Neolithic	Phase IIIa2	Sq A, Quads 2 and 3, Levels 15,16
LJ-2943	6960 ± 80	--	charcoal	Neolithic	Phase IIIc	Sq A, Quad 1, Level 10
LJ-2944	7020 ± 50	--	charcoal	Neolithic	Phase IIIa1	Sq B, Quad 4 Level 18
LJ-3180	7750 ± 60	--	charcoal	Neolithic	Phase IIa2	Sq D, Quad 2, Level 22
LJ-3181	7240 ± 50	--	charcoal	Neolithic	Phase IIa2	Sq D, Quad 2, Level 22
LJ-3182	7920 ± 50	--	charcoal	Neolithic	Phase IIIa1	Sq C, Quad 1, Level 21
LJ-3184	7320 ± 50	--	charcoal	Neolithic	Phase Ib	Sq B, Quad 2, Level 27
LJ-3186	7290 ± 50	--	charcoal	Neolithic	--	Sq B, Area 5, Level 24
LJ-3200	7030 ± 80	--	charcoal	Neolithic	Phase IIIc	Sq D, Quad2, Level II
LJ-3201	7210 ± 90	--	charcoal	Neolithic	Phase IIb	Sq D, Quad 2, Level 19
LJ-3202	7020 ± 100	--	charcoal	Neolithic	Phase IVa	Sq C, Quad 4, Level 9
LJ-3203	6990 ± 70	--	charcoal	Neolithic	Sesklo	Sq D, Quad 4, Level 19, mixed
LJ-3325	7280 ± 50	--	charcoal	Neolithic	Phase IIa2	Sq B, Area 5, Levels 20, 21
LJ-3326	7290 ± 80	--	charcoal	Neolithic	Phase IIb	Sq A, Quad 2, Level 22
LJ-3327	7120 ± 60	--	charcoal	Neolithic	Phase IIIa1	Sq A, Quad 4, Level 21
LJ-3328	7300 ± 50	--	charcoal	Neolithic	Phase IIa2	Sq B, Quad 1, Level 19
LJ-3329	7360 ± 50	--	charcoal	Neolithic	Phase Ib	Sq B, Quad 1, Level 26
LJ-4449	7490 ± 150	--	charcoal	Neolithic		
P-2117	7273 ± 76	--	charcoal	Neolithic	Phase IIa1	Sq A, Quad 1, Level 26
P-2118	7470 ± 175	--	organic	Neolithic	Phase Ia	Sq B, Quad 2, Level 26
P-2120	7340 ± 70	--	charcoal	Neolithic	Phase IIIa1	Sq A, Quad 1, Level 18
P-2121	7180 ± 90	--	charcoal	Neolithic	Phase IIIa2	Sq B, Quad 2, Level 17
P-2122	7110 ± 90	--	charcoal	Neolithic	Phase IIIa2	Sq B, Quad 2, Level 16
P-2123	7450 ± 80	--	charcoal	Neolithic		Zone A-D3 cche 14
P-2123?	7454 ± 78	--	--	Neolithic	Sesklo	Zone A3 cche 14
P-2124	7090 ± 90	--	charcoal	Neolithic	Phase IIIb	Sq A, Quad 2, Level 14
P-2125	6960 ± 90	--	charcoal	Neolithic	Phase III	Sq B, Quad 4, Level 13
P-2128	7270 ± 80	--	charcoal	Neolithic		
P-2130	7080 ± 100	--	charcoal	Neolithic	Phase IVa	Sq D, Quad 2, Level 7

Radiocarbon Data: Tab.7 (cont.) Achilleion (39,25° N, 22,42° E)

Lab-Code	14C-Age [BP]	Material	Period	Phase	Locus	
UCLA-1882A	7084 ± 100	--	Neolithic	Phase IVb	Sq D, Quad 4,	Level 2
UCLA-1882B	7260 ± 155	--	Neolithic	Phase Ib	Sq B, Quad 1,	Level 31
UCLA-1896?	7280 ± 100	--	Neolithic	Sesklo	Zone A-3	cche 14
UCLA-1896A	7460 ± 175	--	Neolithic	Phase Ia	Sq T, Area 7,	Levels 11, 12
UCLA-1896B	7180 ± 55	--	Neolithic	Phase IIIb	Sq A, Quad 1,	Level 13
UCLA-1896C	7330 ± 100	--	Neolithic	Phase IIb	Sq D, Quad 2,	Level 18

Radiocarbon Data: Tab.8 Nea Nikomedeia (40,59 °N, 22,28 °E)

Lab-Code	14C-Age [BP]	δ13C [‰ PDB]	Material	Species	Period	Locus
GX-679	7780 ±270	--	--	-- --	Neolithic	Phase I
OxA-1603	7050 ± 80	--	seeds	Triticum dicoccum	Neolithic	C1 Spit 2A
OxA-1604	7340 ± 90	--	seeds	Triticum dicoccum	Neolithic	C1 Spit 3A
OxA-1605	7400 ± 90	--	seeds	Hordeum vulgare	Neolithic	H6/1a+H7/A
OxA-1606	7400 ±100	--	seeds	Lens culinaris	Neolithic	K6/1FG
OxA-3873	7300 ± 80	--	bone	Ovis	Neolithic	NN D8/2, J358
OxA-3874	7370 ± 80	--	bone	Capra	Neolithic	NN B5/1, L644
OxA-3875	7280 ± 90	--	bone	Sus	Neolithic	NN F6/1 FC PD,0470
OxA-3876	7370 ± 90	--	bone	Bos	Neolithic	--
OxA-4280	6920 ±120	--	seeds	Triticum monococcum	Neolithic	--
OxA-4281	7100 ± 90	--	seeds	Triticum dicoccum	Neolithic	C1 Spit 3A
OxA-4282	7400 ± 90	--	seeds	Hordeum vulgare	Neolithic	--
OxA-4283	7260 ± 90	--	seeds	Lens culinaris	Neolithic	K6/1FG
P-1202	7557 ± 91	--	charcoal	organic fraction	Neolithic	A4/3 Feature A
P-1203A	7281 ± 74	--	organic	organic fraction	Neolithic	--
Q-655	8180 ± 150	--	charcoal	-- --	Neolithic	--

Radiocarbon Data: Tab.9 Junacite (42,2419 °N, 24,2720 °E) Source: Görsdorf and Bojadziev 1996

Lab-Code	14C-Age [BP]	δ13C [‰ PDB]	Material	Period	Layer	Locus
Bln-3665	4100 ± 50	-25.19	wood	Early Bronze Age	Layer 9	Qu. p7, 3.10 m beam on floor
Bln-3666	4070 ± 60	--	grain	Early Bronze Age	Layer 9	Qu.p7, 3.10 m beam on floor
Bln-3667	4050 ± 50	--	charcoal	Early Bronze Age	Layer 9	Qu. L9, 3.10 m beam from roof
Bln-3668	3830 ± 60	--	lens	Early Bronze Age	Layer 10	Qu. C8, 3.35 m house 10, pithos
Bln-3669	4090 ± 50	--	grain	Early Bronze Age		Layer 10 Qu. U8 3.35 m from pithos
Bln-3670	3990 ± 50	--	peas	Early Bronze Age		Layer 11 Qu. C7/C8 3.70 m house 11, pithos
Bln-3679	4000 ± 70	--	peas	Early Bronze Age	Layer 11	Qu. C7/C8 3.70 m house 11, pithos
Bln-3671	4180 ± 50	--	grain	Early Bronze Age	Layer 13	4.30 m house 22, pithos
Bln-3672	4040 ± 50	--	charcoal	Early Bronze Age	Layer 13	4.30 m house 22, pithos
Bln-3672A	4040 ± 50	--	charcoal	Early Bronze Age	Layer 13	4.30 m house 22, pithos
Bln-3673	3990 ± 60	--	grain	Early Bronze Age	Layer 13	Qu. E9, 4.45 m house 20
Bln-3674	4020 ± 60	--	grain	Early Bronze Age	Layer 13	Qu. E9 4.45 m, house 20
Bln-3675	4280 ± 60	-24,60	grain	Early Bronze Age		Layer 15 house 31, from floor, 4.66 m
Bln-3676	4030 ± 70	--	grain	Early Bronze Age	Layer 15	house 31, from floor, 4.66 m
Bln-3677	4080 ± 70	--	grain	Early Bronze Age	Layer 15	house 34, 4.64 m
Bln-3678	4050 ± 50	--	grain	Early Bronze Age	Layer 15	house 34, 4.64 m
Bln-3663	4100 ± 50	--	grain	Early Bronze Age	Layer 8	Qu. O8/M6 2,80 m, pithos
Bln-3664	4140 ± 50	-25,25	grain	Early Bronze Age	Layer 8	Qu. O8/M6 2,80 m, pithos
Bln-3662	3910 ± 60	--	acorns	Early Bronze Age	Layer 7	Qu. O9 2,50-2,60 m, pithos
Bln-3660	3970 ± 50	--	charcoal	Early Bronze Age	Layer 6	Qu. 3 9/K6 2,35 m
Bln-3661	4060 ± 60	--	charcoal	Early Bronze Age	Layer 6	Qu. 3 9/K6 2,35 m
Bln-3658	3780 ± 50	--	acorns	Early Bronze Age	Layer 5	Qu. O6/O9 1,95 m, pithos
Bln-3659	3780 ± 50	-25.05	acorns	Early Bronze Age	Layer 5	Qu. O6/O9 1,95 m, pithos
Bln-3657	3760 ± 50	--	acorns	Early Bronze Age	Layer 4	Qu. 3 9, 1.70 m
Bln-3656	3760 ± 50	--	acorns	Early Bronze Age	Layer 3	Qu. K6, 1.45 m, floor

Radiocarbon Data: Tab.10 Ezero (42,48 °N, 25,97 °E) Source: Görsdorf and Bojadziev 1996

Abbreviations: EBA=Early Bronze Age, CH=Chalcolithic, K- = Karanovo, Hor=Horizont
ch = charcoal, gr/ch = grain & charcoal

Lab-Code	14C-Age [BP]	δ13C [‰ PDB]	Material	Period	Period	Horizont	Square	Depth	Repeat Measurements
Bln-1103	4280 ± 100	--	ch	EBA	K-VII	I-7	Qu.D1	1.65 m	Bln-523, Bln-1103, Bln-1826
Bln-1155	3040 ± 100	--	ch	EBA	K-VII	I-13	Qu.C6 I-13	3.35 m	Bln-1840, Bln-1155, Bln-1256
Bln-1156	3980 ± 100	--	ch	EBA	K-VII	I-13	Qu.D11/D12	3.35 m	Bln-1156, Bln-1841
Bln-1158	4363 ± 100	--	ch	EBA	K-VII	I-13	Qu.D8	3.35 m	Bln-1158, Bln-1786
Bln-1159	4099 ± 100	--	ch	EBA	K-VII	I-13	Qu.D11	3.35 m	Bln-1843, Bln-1920, Bln-1920B
Bln-1256	4300 ± 80	--	ch	EBA	K-VII	I-13	Qu.C6 I-13	3.35 m	Bln-1840, Bln-1155, Bln-1256
Bln-1786	4450 ± 85	--	ch	EBA	K-VII	I-13	Qu.D8	3.35 m	Bln-1158, Bln-1786
Bln-1822	4275 ± 65	--	ch	EBA	K-VII	I-6	Qu.A7	1.30 m	Bln-422, Bln-1822
Bln-1824	4135 ± 65	--	grain	EBA	K-VII	I-4	Qu.C10	0.70 m	Bln-429, Bln-1824
Bln-1825	4290 ± 50	--	ch	EBA	K-VII	I-7	Qu.D	1.55 m	Bln-522, Bln-1825
Bln-1826	4310 ± 45	--	ch	EBA	K-VII	I-7	Qu.D1	1.65 m	Bln-523, Bln-1103, Bln-1826
Bln-1827	4475 ± 60	--	grain	EBA	K-VII	I-7	Qu.E4	1.65 m	Bln-524, Bln-1827
Bln-1828	4400 ± 50	--	ch	EBA	K-VII	I-7	Qu.B3	1.75 m	Bln-525, Bln-1828
Bln-1829	4165 ± 40	--	ch	EBA	K-VII	I-7	Qu.D10	1.60 m	Bln-526, Bln-1829
Bln-1830	4335 ± 45	--	gr/ch	EBA	K-VII	I-8	Qu.A6	1.60 m	Bln-527, Bln-1830

Radiocarbon Data: Tab.10 (cont) Ezero (42,48 °N, 25,97 °E) Source: Görsdorf and Bojadziev 1996

Abbreviations: EBA=Early Bronze Age, CH=Chalcolithic, K- = Karanovo, Hor=Horizont
ch = charcoal, gr/ch = grain & charcoal

Lab-Code	14C-Age [BP]	δ13C [‰ PDB]	Material	Period	Period	Horizont	Square	Depth	Repeat Measurements
Bln-1831	4360 ± 60		ch	EBA	K-VII	I-8	Qu.A6	1.80 m	Bln-528, Bln-1831
Bln-1832	4245 ± 50		ch	EBA	K-VII	I-8	Qu.B	1.80 m	Bln-529, Bln-1832
Bln-1834	4420 ± 60		gr/ch	EBA	K-VII	I-9	Qu.E11	2.20 m	Bln-722, Bln-1834
Bln-1835	4260 ± 45		grain	EBA	K-VII	I-10	Qu.C11	2.45 m	Bln-727, Bln-1835
Bln-1836	4160 ± 55		ch	EBA	K-VII	I-12	Qu.B1	3.05 m	Bln-903, Bln-1836
Bln-1837	4415 ± 40		ch	EBA	K-VII	I-13	Qu.E7/E6	3.20 m	Bln-904, Bln-1837
Bln-1838	4305 ± 65		gr/ch	EBA	K-VII	I-13	Qu.E5	3.20 m	Bln-905, Bln-1838
Bln-1840	4590 ± 100		ch	EBA	K-VII	I-13	Qu.C6	3.35 m	Bln-1840, Bln-1155, Bln-1256
Bln-1841	4420 ± 50		ch	EBA	K-VII	I-13	Qu.D11/D12	3.45 m	Bln-1156, Bln-1841
Bln-1843	4430 ± 50		ch	EBA	K-VII	I-13	Qu.D11	3.35 m	Bln-1843, Bln-1920, Bln-1920B
Bln-1920	4390 ± 50		ch	EBA	K-VII	I-13	Qu.D11	3.35 m	Bln-1843, Bln-1920, Bln-1920B
Bln-1920B	4500 ± 50		ch	EBA	K-VII	I-13	Qu.D11	3.35 m	Bln-1843, Bln-1920, Bln-1920B
Bln-421	4335 ± 80		gr/ch	EBA	K-VII	I-6	Qu.D8	1.30 m	
Bln-422	4310 ± 80		ch	EBA	K-VII	I-6	Qu.A7	1.30 m	Bln-422, Bln-1822
Bln-423	4440 ± 80		ch	EBA	K-VII	I-7	Qu.E5	1.35 m	
Bln-424	4575 ± 80		ch	EBA	K-VII	I-7	Qu.C4	1.35 m	
Bln-427	4365 ± 80		ch	EBA	K-VII	I-6	Qu.D10	0.80 m	
Bln-428	4260 ± 80		grain	EBA	K-VII	I-4	Qu.D10	0.80 m	
Bln-429	4130 ± 100		gr/ch	EBA	K-VII	I-4	Qu.C10	0.70 m	Bln-429, Bln-1824
Bln-522	4455 ± 100		ch	EBA	K-VII	I-7	Qu.D5	1.55 m	Bln-522, Bln-1825
Bln-523	4400 ± 100		ch	EBA	K-VII	I-7	Qu.D1	1.65 m	Bln-523, Bln-1103, Bln-1826
Bln-524	4460 ± 100		grain	EBA	K-VII	I-7	Qu.E4	1.65 m	Bln-524, Bln-1827
Bln-525	4280 ± 100		ch	EBA	K-VII	I-7	Qu.B3	1.75 m	Bln-525, Bln-1828
Bln-526	4135 ± 100		ch	EBA	K-VII	I-7	Qu.D10	1.60 m	Bln-526, Bln-1829
Bln-527	4390 ± 80		grain	EBA	K-VII	I-8	Qu.A6	1.60 m	Bln-527, Bln-1830
Bln-528	4445 ± 100		ch	EBA	K-VII	I-8	Qu.A6	1.80 m	Bln-528, Bln-1831
Bln-529	4375 ± 100		ch	EBA	K-VII	I-8	Qu.B7	1.80 m	Bln-529, Bln-1832
Bln-722	4285 ± 100		grain	EBA	K-VII	I-9	Qu.E11	2.20 m	Bln-722, Bln-1834
Bln-724	4365 ± 150		grain	EBA	K-VII	I-9	Qu.C10	2.05 m	
Bln-725	4120 ± 100		grain	EBA	K-VII	I-10	Qu.A9	2.45 m	
Bln-726	4285 ± 100		grain	EBA	K-VII	I-10	Qu.C9	2.45 m	
Bln-727	4315 ± 100		grain	EBA	K-VII	I-10	Qu.C11	2.45 m	Bln-727, Bln-1835
Bln-902	4360 ± 100		ch	EBA	K-VII	I-11	Qu.A7	2.70 m	
Bln-903	3935 ± 100		ch	EBA	K-VII	I-12	Qu.B1	3.05 m	Bln-903, Bln-1836
Bln-904	4143 ± 100		ch	EBA	K-VII	I-13	Qu.E7/E6	3.20 m	Bln-904, Bln-1837
Bln-905	4113 ± 100		gr/ch	EBA	K-VII	I-13	Qu.E5	3.20 m	Bln-905, Bln-1838
Bln-1157	5474 ± 100		ch	CH	K-V/VI	II-14	Qu.B8/C8	3.45 m	Bln-1157, Bln-1157A, Bln-1240
Bln-1157A	4897 ± 350		ch	CH	K-V/VI	II-14	Qu.B8/C8	3.45 m	Bln-1157, Bln-1157A, Bln-1240
Bln-1240	5752 ± 100		ch	CH	K-V/VI	II-14	Qu.B8/C8	3.45 m	Bln-1157, Bln-1157A, Bln-1240
Bln-1823	5740 ± 70		grain	CH	K-V/VI	II-15	Qu.SW-Sector	4.30 m	Bln-425, Bln-1823
Bln-1833	6415 ± 70		ch	CH	K-IV	III-24	SW-Sect .	7.30 m	Bln-530, Bln-1833
Bln-425	5580 ± 80		grain	CH	K-VI	II-15	SW-Sect.	4.30 m	Bln-425, Bln-1823
Bln-530	6270 ± 80		ch	CH	K-IV	III-24	SW-Sect.	7.30 m	Bln-530, Bln-1833

Radiocarbon Data: Tab.11 Drama-Merdzumekja (42.23° N, 26,43 °E) Source: Thomas & Gleser 2011

Lab-Code	14C-Age [BP]	δ13C [‰ PDB]	Material	Speciesl	Period	Locus
Bln-5115	5554 ± 38	-20.42	bone	animal	Karanovo V	Areal H16, Graben 687
Bln-5116	4941 ± 38	-18.61	bone	animal	Transitional	Areal H08, Kreisgraben
Bln-5117	5587 ± 35	-19.63	bone	animal	Karanovo VI	--
Erl-12296	5739 ± 48	-18.50	bone	bos	Karanovo V/VI	Areal F13, house 486
Erl-12297	5636 ± 49	-19.50	bone	goat	Karanovo V/VI	Areal F13, house 486
Erl-12298	5680 ± 48	-19.90	bone	pig	Karanovo V/VI	Areal F13
Erl-12299	4898 ± 45	-22.00	bone	pig	Transitional	Areal L10, house 244
Erl-12300	5768 ± 46	-20.40	bone	pig	Neolithic	Areal L10, house 244
Erl-12301	5839 ± 47	-20.00	bone	pig	Neolithic	Areal L10
Erl-14434	5602 ± 57	-21.50	bone	animal	Neolithic	--
Erl-14435	5677 ± 54	-20.40	bone	animal	Karanovo VI	Areal Q1
Erl-14436	5687 ± 58	-20.10	bone	animal	Karanovo VI	Areal Q13
Erl-14437	4629 ± 53	-21.60	bone	animal	Cernavoda III	Areal Q12
Erl-14438	4626 ± 55	-20.80	bone	animal	Cernavoda III	Areal Q12
Erl-14439	5562 ± 59	-20.90	bone	animal	Karanovo VI	Areal Q12
Erl-14440	5667 ± 56	-21.30	bone	animal	Karanovo VI	Areal P11
Erl-14441	4751 ± 57	-20.80	bone	animal	Cernavoda III	Areal R09
Erl-14442	4575 ± 62	-21.00	bone	animal	Cernavoda III	Areal R13
Erl-14443	4592 ± 57	-20.20	bone	animal	Cernavoda III	Areal Q11

Radiocarbon Data: Tab.12 Varna (43,21 °N, 27,91 °E), Higham et al., 2008

Lab-Code	14C-Age [BP]	δ13C [‰ PDB]	Material /Species	Period	Period	Locus
OxA-13687	5569 ± 32	-19,10	bone/human	Chalcolithic	KGK VI	Burial 10
OxA-13686	5639 ± 32	-19,30	bone/human	Chalcolithic	KGK VI	Burial 11
OxA-13685	5720 ± 29	-18,50	bone/human	Chalcolithic	KGK VI	Burial 43
OxA-13692	5657 ± 30	-19,10	bone/human	Chalcolithic	KGK VI	Burial 44
OxA-13250	5626 ± 31	-19,30	bone/human	Chalcolithic	KGK VI	Burial 94
OxA-13646	5757 ± 34	-19,40	bone/animal	Chalcolithic	KGK VI	Burial 111
OxA-13865	5855 ± 34	-18,30	bone/human	Chalcolithic	KGK VI	Burial 111
OxA-13251	5702 ± 32	-18,60	bone/human	Chalcolithic	KGK VI	Burial 112
OxA-13848	5766 ± 36	-19,00	bone/human	Chalcolithic	KGK VI	Burial 117
OxA-13811	5530 ± 36	-20.20	bone/animal	Chalcolithic	KGK VI	Burial 117
OxA-13252	5672 ± 34	-18,90	bone/human	Chalcolithic	KGK VI	Burial 121
OxA-13253	5685 ± 33	-18,60	bone/human	Chalcolithic	KGK VI	Burial 125
OxA-13694	5654 ± 36	-19,80	bone/human	Chalcolithic	KGK VI	Burial 137
OxA-13689	5690 ± 32	-19,70	bone/human	Chalcolithic	KGK VI	Burial 143
OxA-13690	5700 ± 30	-19,70	bone/animal	Chalcolithic	KGK VI	Burial 143
OxA-13688	5787 ± 30	-18,90	bone/human	Chalcolithic	KGK VI	Burial 158
OxA-13691	5668 ± 32	-19,80	bone/human	Chalcolithic	KGK VI	Burial 215
OxA-13693	5660 ± 29	-19,80	bone/human	Chalcolithic	KGK VI	Burial 225
OxA-13254	5732 ± 33	-18,60	bone/human	Chalcolithic	KGK VI	Burial 25

Radiocarbon Data: Tab.13 Azmak (42,45 °N, 25,42 °E)

Lab-Code	14C-Age [BP]	δ13C [‰ PDB]	Material	Species	Period	Period	Locus
Bln-131	5683 ± 100	--	charcoal	--	Neolithic	Karanovo VI	--
Bln-134	5546 ± 200	--	charcoal	--	Neolithic	Karanovo VI	--
Bln-135	5689 ± 100	--	charcoal	--	Neolithic	Karanovo VI	--
Bln-149	5888 ± 100	--	seeds	--	Neolithic	Karanovo VI	--
Bln-138	5618 ± 200	--	charcoal	--	Neolithic	Karanovo VI	--
Bln-139	5698 ± 100	--	seeds	--	Neolithic	Karanovo VI	--
Bln-144	5592 ± 120	--	seeds	--	Neolithic	Karanovo VI	--
Bln-145	5387 ± 100	--	seeds	--	Neolithic	Karanovo VI	I/10
Bln-146	5006 ± 150	--	seeds	--	Neolithic	Karanovo VI	--
Bln-141	5642 ± 100	--	seeds	--	Neolithic	Karanovo VI	--
Bln-142	5793 ± 150	--	seeds	--	Neolithic	Karanovo V	--
Bln-143	5729 ± 150	--	seeds	--	Neolithic	Karanovo V	--
Bln-136	5840 ± 100	--	grain	--	Neolithic	Karanovo V	--
Bln-137	5697 ± 100	--	charcoal	--	Neolithic	Karanovo V	--
Bln-147	5214 ± 150	--	seeds	--	Neolithic	Karanovo V	--
Bln-148	5760 ± 150	--	seeds	--	Neolithic	Karanovo V	--
Bln-150	5632 ± 150	--	seeds	--	Neolithic	Karanovo V	--
Bln-151	5807 ± 100	--	seeds	--	Neolithic	Karanovo V	--
Bln-140A	6476 ± 100	--	seeds	--	Neolithic	Karanovo II/III	--
Bln-203	6870 ± 100	--	charcoal	Quercus sp.	Neolithic	Karanovo I	burned layer E-side of central profile
Bln-224	6650 ± 150	--	grain	Triticum	Neolithic	Karanovo I	central profile Ia/8
Bln-267	6758 ± 100	--	charcoal	--	Neolithic	Karanovo I	burned layer E-side of central profile
Bln-291	7158 ± 150	--	charcoal	Quercus sp.	Neolithic	Karanovo I	Square B84 (or B99 ?)
Bln-292	6878 ± 100	--	seeds	Triticum	Neolithic	Karanovo I	Square A84 I/12
Bln-293	7303 ± 150	--	charcoal	Quercus sp.	Neolithic	Karanovo I	Square W85; Level I-1
Bln-294	6768 ± 100	--	charcoal	Quercus sp.	Neolithic	Karanovo I	Square W85
Bln-295	6720 ± 100	--	seeds	Triticum	Neolithic	Karanovo I	Square W83
Bln-296	6779 ± 100	--	charcoal	Quercus sp.	Neolithic	Karanovo I	Square B99
Bln-297	6675 ± 100	--	seeds	Triticum	Neolithic	Karanovo I	Square A100
Bln-298	6540 ± 100	--	charcoal	Quercus sp.	Neolithic	Karanovo I	Square A100
Bln-299	6812 ± 100	--	charcoal	Fraxinus	Neolithic	Karanovo I	Square B99
Bln-300	6426 ± 150	--	charcoal	Quercus sp	Neolithic	Karanovo I	Square B132
Bln-301	6483 ± 100	--	charcoal	Quercus sp.	Neolithic	Karanovo I	Square G70
Bln-430	6279 ± 120	--	seeds	--	Neolithic	Karanovo I	Square A85

Radiocarbon Data: Tab.14 Drama-Gerena (42.24 °N, 26,43° E) Gleser, 2011

Lab-Code	14C-Age [BP]	δ13C [‰ PDB]	Material	Species	Period	Locus
Bln-5112	6257 ± 40	-20.67	bone	animal	Gerena B1/B2	Areal TG01/Area B
Bln-5113	6192 ± 41	-21.39	bone	animal	Karanovo IV	Areal TG01/Area A
Erl-12310	6381 ± 47	-19.90	bone	Bos/Ur	Neolithic	Areal TG01/Area A
Erl-12311	6456 ± 48	-19.40	bone	Bos	Gerena B1/C	Areal TG01/Area A
Erl-12312	6474 ± 48	-19.00	bone	Bos	Karanovo III-IV	Areal TG01/Area A, Grube B
Erl-12313	6436 ± 48	-18.00	bone	Bos	Karanovo III-IV	Areal TG01/Area A, Grube B
Erl-12314	6474 ± 50	-20.00	bone	Ur	Neolithic	--
Erl-12315	6411 ± 50	-20.20	bone	animal	Neolithic	Areal TG01/Area A1
Erl-12316	6319 ± 50	-19.70	bone	pig	Karanovo III/IV	Areal TG01/Area A, Grube B
Erl-12317	6385 ± 50	-20.30	bone	sheep	Karanovo III/IV	Areal TG01/Area A, Grube B

Radiocarbon Data: Tab.15 Kremenik (42.30 °N, 23.26 °E)
Source: Görsdorf and Bojadziev, 1996

Lab-Code	14C-Age [BP]	δ13C [‰ PDB]	Material	Period	Horizont	Locus		Depth
Bln-2105	6530 ± 50	--	charcoal	Neolithic	Hor.3	Qu. P15,	inside house,	7.05 m
Bln-2106	6475 ± 40	--	charcoal	Neolithic	Hor.3	Qu. P15	inside house, near oven	7.02 m
Bln-2549	6350 ± 60	--	charcoal	Neolithic	Hor.4	Qu. P16,	--	7.77 m
Bln-2550	6550 ± 60	--	charcoal	Neolithic	Hor.4	Qu. P16,	--	7.75 m
Bln-2551	6450 ± 100	--	charcoal	Neolithic	Hor.4	Qu. P13,	oven	7.47 m
Bln-2552	6460 ± 60	--	charcoal	Neolithic	Hor.2	Qu. Q15,	inside pithos	7.40 m
Bln-2553	6660 ± 60	--	charcoal	Neolithic	Hor.3	Qu. P15,	oven,	7.50 m
Bln-2554	6620 ± 100	--	charcoal	Neolithic	Hor.2	Qu. P12,	house floor,	6.47 m
Bln-2555	6840 ± 60	--	charcoal	Neolithic	Hor.3	Qu. P14,	house floor,	7.10 m
Bln-2556	6480 ± 60	--	charcoal	Neolithic	Hor.3	Qu. P14,	house floor	7.10 m

Radiocarbon Data: Tab.16 Karanovo (42.55°N, 25.87°E)
Source: Görsdorf and Bajadziev (1996), Hiller (1989)

Lab-Code	14C-Age [BP]	δ13C [‰ PDB]	Material	Period	Locus		Depth	Repeat Measurement
Bln-154	5830 ± 250	--	grain	Karanovo VI	Sector VI , house	--	2.70 m	--
Bln-1182	5520 ± 100	--	grain	Karanovo V	--	--	5.50 m	--
Bln-153	5625 ± 100	-25.00	grain	Karanovo V	--	--	5.50 m	--
Bln-158	6395 ± 100	-22.70	grain	Karanovo III	Sector IV , NE-side of tell		8.90 m	--
Bln-3458	6440 ± 60	--	charcoal	Karanovo III	Qu.P 18/II	--	210.00 m	--
Hv-14180	6230 ± 75	--	charcoal	Karanovo III	Qu.P 18/II	--	210.00 m	id Bln-3458
Bln-3459	6420 ± 60	--	charcoal	Karanovo III	Qu.P 18/II	--	210.00 m	--
Hv-14181	6530 ± 75	--	charcoal	Karanovo III	Qu.P 18/II	--	210.00 m	id Bln-3459
Bln-3460	6440 ± 60	--	charcoal	Karanovo III	Qu.P 18/II	--	210.00 m	--
Hv-14182	6355 ± 75	--	charcoal	Karanovo III	Qu.P 18/II	--	210.00 m	id Bln-3460
Bln-3461	6480 ± 60	--	charcoal	Karanovo III	Qu.P 18/II, beam	--	210.00 m	--
Hv-14184	6340 ± 75	--	charcoal	Karanovo III	Qu.P 18/II, beam	--	210.00 m	id Bln-3461
Bln-3462	6510 ± 60	--	charcoal	Karanovo III	Qu. P 18/II 2	--	10.00 m	--
Hv-14186	6475 ± 65	--	charcoal	Karanovo III	Qu. P 18/II	--	210.00 m	id Bln-3462
Bln-3463	6350 ± 60	--	seeds	Karanovo III	Qu. P 18/II	--	210.00 m	--
Hv-14183	6420 ± 60	--	seeds	Karanovo III	Qu. P 18/II	--	210.00 m	id Bln-3463
Bln-3464	6500 ± 50	--	seeds	Karanovo III	Qu. P 18/II	--	210.00 m	--
Hv-14185	5895 ±115	--	seeds	Karanovo III	Qu. P 18/II	--	210.00 m	id Bln-3464
Bln-3465	6410 ± 60	--	seeds	Karanovo III	Edge of tell	--	210.00 m	--
Bln-3585	6130 ± 60	-25.21	charcoal	Karanovo III	Qu.Q 18/I	--	209.35-209.05 m	--
Hv-14609	6535 ± 70	--	charcoal	Karanovo III	Qu.Q 18/I	--	209.35-209.05 m	id Bln-3585
Bln-3587	6380 ± 60	--	seeds	Karanovo III	Qu. P 18/II	--	210.20 m	--
Hv-14611	6555 ± 60	--	seeds	Karanovo III	Qu. P 18/II	--	210.20 m	id Bln-3587
Bln-3717	6450 ± 60	--	seeds	Karanovo III	Qu.Q 17/II	--	210.20 m	--
Bln-3717H	6510 ± 60	--	humic acid	Karanovo III	Qu. Q 17/II	--	210.20 m	--
Bln-3904	6375 ± 70	-25.68	- charcoal	Karanovo III	Qu. Q 18/I	--	209.35-209.05 m	--
Bln-3941	6750 ± 50	-25.33	charcoal	Karanovo II	Qu. P 19/IV, NE-corner		207.65-207.60 m	--
Bln-3943	6760 ± 50	-26.05	charcoal	Karanovo II	Qu. P 19/III, oven Osthaus III		207.50-207.45 m	--
Bln-3944	6785 ± 60	-25.26	charcoal	Karanovo II	Qu. P19/III oven Haus V.2		--	--
Bln-3716	6910 ± 60	--	charcoal	Karanovo II	Qu. Q17/II	--	209.35-209.20 m	--
Bln-3716H	6850 ± 60	--	humic acids	Karanovo II	Qu. Q17/II	--	209.35-209.20 m	--
Bln-201	6540 ± 100	-27.00	charcoal	Karanovo II	Sector III	--	--	--
Bln-234	6490 ± 150	-25.90	charcoal	Karanovo II	Sector III	--	--	
Bln-3586	6780 ± 60	--	charcoal	Karanovo II	Qu Q 17/II	--	209.35-209.20 m	--
HV-14610	6800 ± 75	--	charcoal	Karanovo II	Qu Q 17/II	--	209.35-209.20 m	id Bln-3586
Bln-152	6807 ± 100	--	charcoal	Karanovo II	Sector III, SW-side of tell		--	--
Bln-3942	6820 ± 50	--	charcoal	Karanovo I	Qu.Q 17/IV	--	207.5 m	--
Bln-4177	7110 ± 50	-25.22	charcoal	Karanovo I	Qu. P 18/III	--	207.30-207.25 m	--
Bln-4178	6730 ± 80	--	charcoal	Karanovo I	Qu. P 19/III , oven	--	207.40 m	--
Bln-4179	7130 ± 70	--	charcoal	Karanovo I	Qu. Q 18/I	--	207.40 m	--
Bln-4334	3810 ± 45	-25.25	charcoal	Karanovo I	Qu. P 19/I	--	--	--
Bln-4335	6710 ± 55	-25.46	charcoal	Karanovo I	Qu. Q 19/II	--	207.04-206.93 m	--
Bln-4336	7110 ± 50	-26.46	charcoal	Karanovo I	Qu. P 19/III	--	207.05 m	--
Bln-4337	6810 ± 65	-26.21	charcoal	Karanovo I	Qu. Q 19/II	--	206.9 m	--
Bln-4338	6955 ± 45	-24.25	charcoal	Karanovo I	Qu. P 18/IV	--	207.00 m	--
Bln-4339	7090 ± 90	--	charcoal	Karanovo I	Qu. Q 19/III-IV	--	--	--

Radiocarbon Data: Tab.17 Cavdar (42,63 °N, 24,08 °E)

Lab-Code	14C-Age [BP]	δ13C [‰ PDB]	Material	Period		Locus	Level
Bln-906	6720 ± 100	--	charcoal	Neolithic	Karanovo I	Square G11,	Level II
Bln-1030	6760 ± 100	--	peas	Neolithic	Karanovo I	Square F15,	Level III
Bln-907	6320 ± 100	--	peas	Neolithic	Karanovo I	Square F15,	Level III
Bln-908	6990 ± 150	--	charcoal	Neolithic	Karanovo I	Square I10,	Level III
Bln-909	6815 ± 100	--	charcoal	Neolithic	Karanovo I	Square J11,	Level III
Bln-910	6665 ± 100	--	charcoal	Neolithic	Karanovo I	Square J11,	Level III
Bln-910A	6555 ± 100	--	charcoal	Neolithic	Karanovo I	Square J11,	Level III
Bln-911	6870 ± 120	--	charcoal	Neolithic	Karanovo I	Square K13,	Level III
Bln-998	7045 ± 120	--	charcoal	Neolithic	Karanovo I	Square I10,	Level III
Bln-1160	6680 ± 100	--	charcoal	Neolithic	Karanovo I	Square H15,	Level IV
Bln-1160A	7040 ± 100	--	charcoal	Neolithic	Karanovo I	Square H15,	Level IV
Bln-1162	6400 ± 100	--	charcoal	Neolithic	Karanovo I	Square G16,house,	Level IV
Bln-1162A	6985 ± 100	--	charcoal	Neolithic	Karanovo I	Square G16,house,	Level IV
Bln-1241	6852 ± 100	--	charcoal	Neolithic	Karanovo I	Square J14,	Level IV
Bln-1241A	6930 ± 100	--	charcoal	Neolithic	Karanovo I	Square J14,	Level IV
Bln-1251	6997 ± 100	--	charcoal	Neolithic	Karanovo I	Square G16,	Level IV
Bln-4106	6840 ± 50	--	charcoal	Neolithic	Karanovo I	Square O14,	Level V
Bln-4261	7120 ± 80	--	charcoal	Neolithic	Karanovo I	Square P14,	Level V
Bln-1578	6994 ± 55	--	charcoal	Neolithic	Karanovo I	Square G16,house,	Level VI
Bln-1579	7003 ± 45	--	charcoal	Neolithic	Karanovo I	Square G14	Level VI
Bln-1580	7202 ± 55	--	charcoal	Neolithic	Karanovo I	Square G14,	Level VI
Bln-1581	7000 ± 60	--	charcoal	Neolithic	Karanovo I	Square G15,	Level VI
Bln-1582	7020 ± 45	--	charcoal	Neolithic	Karanovo I	Square F15	Level VI
Bln-1583	7208 ± 52	--	charcoal	Neolithic	Karanovo I	Square F16,	Level VI
Bln-1663	7070 ± 50	--	charcoal	Neolithic	Karanovo I	Square G15,	Level VI
Bln-2107	6550 ± 50	--	charcoal	Neolithic	Karanovo I	Square B13,	Level VI
Bln-2108	7195 ± 65	--	charcoal	Neolithic	Karanovo I	Square C15/C16,	Level VI
Bln-2662	6820 ± 50	--	charcoal	Neolithic	Karanovo I	Square A15,	Level VI

Radiocarbon Data: Tab.18 Baile Herculane (44.87 °N, 22.41° E), Laszlo 1997

Lab-Code	14C-Age [BP]	δ13C [‰ PDB]	Material	Period	Phase	Locus
Lj-3533	4460 ± 100	--	--	Early Bronze Age	Cotofeni IIB	--
Lj-3534	4360 ± 100	--	--	Early Bronze Agen	Cotofeni IIIC	--
LJ-3535	4350 ± 60	--	--	Early Bronze Age	Cotofeni IIIC	Layer 5
LJ-3536	4300 ± 60	--	--	Early Bronze Age	Cotofeni	--
Lj-3536	4300 ± 60	--	--	Early Bronze Age	Cotofeni IIIC	--

Radiocarbon Data: Tab.19 Cernavoda

Lab-Code	14C-Age [BP]	δ13C [‰ PDB]	Material	Species	Period	Phase	Locus
Bln-60	4260 ± 100	--	--	--	Transitional	Cernavoda I	--
Bln-61	4385 ± 100	--	charcoal	--	Transitional	Cernavoda I	--
Bln-62	4260 ± 100	--	charcoal	Quercus	--	Cernavoda I	--

Radiocarbon Data: Tab.20 Draguseni (46.91 °N, 27,50 °E) Laszlo 1997

Lab-Code	14C-Age [BP]	δ13C [‰ PDB]	Material	Phase	Locus
Bln-1060	5355 ± 100	--	charcoal	Cucuteni A3	--
Bln-1194	5205 ± 100	--	charcoal	Cucuteni A4	--
Bln-1195	5430 ± 100	--	charcoal	Cucuteni A4	--
HD-14544	5188 ± 18	--	bone	Cucuteni A-B1	1961, 6-10
HD-14761	5246 ± 24	--	bone	Cucuteni A-B1--	1963, e-f, -1-1.10 m
HD-14831	4996 ± 26	--	bone	Cucuteni A-B1--	1961, complex V,-0.20 m

Radiocarbon Data: Tab.21 Scanteia (46.91 °N, 27.56 °E), Lazarovici 2010

Lab-Code	14C-Age [BP]	δ13C [‰ PDB]	Material	Species	Phase	Locus
Gd-4685	5750 ± 110	--	bone	--	Cucuteni A3	Section VI,13, -0.62 m
Gd-6387	6320 ± 110	--	bone	--	Cucuteni A3	Cassette 3,3,H4, -0.60-0.70 m
Gd-6388	5330 ± 110	--	bone	--	Cucuteni A3	Section VI,14, -0.55 m
HD-14701	5388 ± 18	--	bone	human	Cucuteni A3	S VIII, Cassette 1, Grave 1, -0.82 m, child
HD-14792	5370 ± 26	--	bone	human	Cucuteni A3	S VIII, Cassette 1, Grave 1, -0.87 m, woman
Hd-16700	5345 ± 51	--	bone	--	Cucuteni A3	Section VIII,13,Pit 62,-2.25 m
Hd-16701	5205 ± 63	--	bone	--	Cucuteni A3	Section VIII, Cassette 1, 16B-17C, -0.73 m
Hd-19572	5280 ± 27	--	bone	--	Cucuteni A3	S IX,m.37, Pit 7, -1.20 m

Radiocarbon Data: Tab.22 Pietrele (44.06 °N, 26.11 °E)

Lab-Code	14C-Age [BP]	δ13C [‰ PDB]	Material	Period	Areal	Locus	Sample ID
Bln-5617	5500 ± 39	-22.10	bone	KGK-VI	B1	house	P02/B/010
Bln-5618	5500 ± 34	-22.20	bone	KGK-VI	B1	house	P02/B/010
Bln-5619	5361 ± 35	-21.70	bone	KGK-VI	B1	house	P02/B/033
Bln-5620	5404 ± 32	-22.10	bone	KGK-VI	B1	house	P02/B/039
Bln-5716	5328 ± 39	-24.70	bone	KGK-VI	F1	central house	P04/F/016
Bln-5717	5366 ± 34	-25.50	grain	KGK-VI	F1	central house	P04/F/016
Bln-5718	5443 ± 38	-24.80	grain	KGK-VI	F1	central house	P04/F/016
Bln-5719	5523 ± 36	-24.60	charcoal	KGK-VI	B1	house	P04/B/043
Bln-5720	5424 ± 33	-25.10	charcoal	KGK-VI	F1	central house in Area F	P04/F/003
Bln-5721	5452 ± 37	-25.20	charcoal	KGK-VI	B1	S of burnt W house of Area B	P04/B/042
Bln-5844	5641 ± 37	-25.60	charcoal	KGK-VI	B1	house in the SW of Area B	P05/B/160
Bln-5845	5574 ± 36	-25.00	charcoal	KGK-VI	B1	house in the W of Area B (wall)	P05/B/159
Bln-5846	5503 ± 49	-25.60	charcoal	KGK-VI	B2	house in the E of Area B	P05/B/158
Bln-5847	5602 ± 47	-24.50	charcoal	KGK-VI	F2	under central house in	P05/F/142
Bln-5930	5478 ± 36	-26.00	charcoal	KGK-VI	F3	lower burnt central house N-part	P06/F/366
Bln-5931	5515 ± 38	-27.80	charcoal	KGK-VI	B3	New structure of a house under fill	P06/B/309
Bln-5932	5473 ± 32	-25.90	charcoal	KGK-VI	F3	lower burnt central house N-part	P06/F/372
Bln-5933	5522 ± 34	-26.90	charcoal	KGK-VI	B3	New structure of a house under fill	P06/B/309
KIA-29315	5520 ± 30	-21.05	bone	KGK-VI	F2	under the burnt central house	P04/F/032
KIA-29316	5605 ± 34	-23.78	charcoal	KGK-VI	B2	unburnt house in the East	P05/B/132
KN-	5538 ± 46	--	charcoal	KGK-VI	B3	unburnt wall of a new house	P07/B/518
KN-	5539 ± 43	--	charcoal	KGK-VI	F3	lower burnt central house (wall)	P07/F/409
KN-	5574 ± 43	--	charcoal	KGK-VI	B3	burnt clay-area; new structures	P07/B/565

Radiocarbon Data: Tab.23 Poduri (46.37 °N, 23.05 °E)

Lab-Code	14C-Age [BP]	δ13C [‰ PDB]	Material	Species	Phase	Locus
Bln-2766	5350 ± 80	--	grain	wheat	Cucuteni A2	H15
Bln-2782	5780 ± 50	--	charcoal	--	Precucuteni III	--
Bln-2783	5690 ± 50	--	charcoal	--	Cucuteni A1 ?	--
Bln-2784	5680 ± 60	--	charcoal	--	Cucuteni A1 ?	--
Bln-2802	5420 ± 150	--	charcoal	--	Cucuteni A2	H2A
Bln-2803	5880 ± 150	--	grain	wheat	Precucuteni III	--
Bln-2804	5820 ± 50	--	charcoal	--	Precucuteni II	--
Bln-2805	5400 ± 70	--	charcoal	--	Cucuteni A2	H2B
Bln-2824	5500 ± 60	--	charcoal	--	Cucuteni A2	H2B
HD-15039	5385 ± 37	--	grain	--	Cucuteni A2	--
HD-15401	5575 ± 35	--	charcoal	--	Cucuteni A2	J4, H66, -1.85 m
Lv-2153	5470 ± 90	--	bone	human	Cucuteni A2	human skull, F1,-1.55 m
HD-15324	5529 ± 29	--	charcoal	--	Cucuteni A2	I2, H66,-1.85 m

Radiocarbon Data: Tab.24 Cascioarele (44.12 °N, 26.46 °E)

Lab-Code	14C-Age [BP]	δ13C [‰ PDB]	Material	Period	Period	Phase
Bln-332	5865 ± 150	--	--	ENeolithic	KGK-VI	Gumelnitsa A2
Bln-332	5865 ± 150	--	--	ENeolithic	KGK-VI	Gumelnitsa A2
Bln-333	5740 ± 120	--	--	ENeolithic	Boian	Boian IV
Bln-334	5750 ± 80	--	--	ENeolithic	Boian	Boian IV
Bln-335	5985 ± 120	--	--	ENeolithic	Boian	Boian IV
Bln-336	5895 ± 120	--	--	ENeolithic	Boian	Boian IV
Bln-343	5485 ± 120	--	--	ENeolithic	KGK-VI	
Bln-343	5485 ± 120	--	--	ENeolithic	KGK-VI	Gumelnitsa A2
Bln-344	5620 ± 120	--	--	ENeolithic	KGK-VI	
Bln-344	5620 ± 120	--	--	ENeolithic	KGK-VI	Gumelnitsa A2
Bln-345	5555 ± 150	--	--	ENeolithic	KGK-VI	
Bln-345	5555 ± 150	--	--	ENeolithic	KGK -VI	Gumelnitsa A2
Bln-598	5855 ± 80	--	--	ENeolithic	Boian	
Bln-598	5955 ± 80	--	--	ENeolithic	Boian	
Bln-599	5670 ± 100	--	--	ENeolithic	Boian	Boian IV
Bln-602	5705 ± 80	--	--	ENeolithic	Boian	Boian IV
Bln-603	5620 ± 100	--	--	ENeolithic	KGK-VI	
Bln-603	5620 ± 120	--	--	ENeolithic	KGK-VI	Gumelnitsa A2
Bln-604	5580 ± 100	--	--	ENeolithic	KGK-VI	
Bln-604	5580 ± 100	--	--	ENeolithic	KGK-VI	Gumelnitsa A2
Bln-605	5675 ± 80	--	--	ENeolithic	KGK-VI	
Bln-605	5675 ± 80	--	--	ENeolithic	KGK-VI	Gumelnitsa A2
Bln-606	5545 ± 100	--	--	ENeolithic	KGK-VI	
Bln-606	5545 ± 100	--	--	ENeolithic	KGK-VI	Gumelnitsa A2
Bln-607	5560 ± 100	--	--	ENeolithic	KGK-VI	
Bln-607	5560 ± 100	--	--	ENeolithic	KGK-VI	Gumelnitsa A2
Bln-608	5400 ± 120	--	--	ENeolithic	KGK-VI	
Bln-608	5400 ± 120	--	--	ENeolithic	KGK-VI	Gumelnitsa A2
Bln-624	5560 ± 100	--	--	ENeolithic	KGK-VI	
Bln-624	5560 ± 100	--	--	ENeolithic	KGK-VI	Gumelnitsa A2
Bln-796	5570 ± 100	--	--	ENeolithic	Boian	Boian IV
Bln-798	5980 ± 100	--	--	ENeolithic	Boian	
Bln-799	5765 ± 100	--	--	ENeolithic	Boian	Boian IV
KN-1149	5705 ± 65	--	--	ENeolithic	Boian	BoianIV

Radiocarbon Data: Tab.25 Parta, Mantu 2000

Lab-Code	14C-Age [BP]	δ13C [‰ PDB]	Material	Period	Phase	Pottery Synchronism
Lv-2138	6160 ± 100	--	--	Neolithic	Banatului II	Vinca-B1-B2
Lv-2139	6330 ± 140	--	--	Neolithic	Banatului II	Vinca B1-B2
Lv-2140	6140 ± 80	--	--	Neolithic	Banatului II	Vinca B1-B2
Lv-2141	6290 ± 80	--	--	Neolithic	Banatului II	Vinca B1-B2
Lv-2142	6240 ± 80	--	--	Neolithic	Banatului	Vinca A3-B1
Lv-2143	6340 ± 100	--	--	Neolithic	Banatului II	Vinca B1-B2
Lv-2144	6100 ± 80	--	--	Neolithic	Banatului II	Vinca B1-B2
Lv-2148	6240 ± 70	--	--	Neolithic	Banatului	Vinca B1-B2
Lv-2149	6160 ± 90	--	--	Neolithic	Banatului II	Vinca B1-B2
Lv-2150	6070 ± 90	--	--	Neolithic	Banatului II	Vinca B1-B2
Lv-2151	6240 ± 70	--	--	Neolithic	Banatului	--
Lv-2145	6560 ± 140	--	--	Neolithic	Banatului I	Vinca A3-B1
Lv-2146	6470 ± 150	--	--	Neolithic	Banatului I	Vinca A3-B1
Lv-2147	6500 ± 130	--	--	Neolithic	Banatului II	Vinca B1-B2

Radiocarbon Data: Tab.26 Dudesti Vechii (46.05 °N, 20.48 °E) Biagi et al. 2005

Lab-Code	14C-Age [BP]	δ13C [‰ PDB]	Material	Species	Period	Period	Phase	Locus	Depth
GrA-24115	6920 ± 80	--	bone	--	Neolithic	Starcevo-Cris	Cris IIIA	Trench 3, Sector A1,	cm 75-80
GrN-28111	6990 ± 50	--	bone	Cervus elaphus	Neolithic	Starcevo-Cris	Cris IIB	Neolithic ditch, Trench 1, Sector E4-5	--
GrN-28113	6930 ± 50	--	bone	Bos sp	Neolithic	Starcevo-Cris	Cris IIB	Trench 3, Sector A2,	cm 165
GrN-28876	6815 ± 70	--	charcoal	Quercus,ulmus	Neolithic	Starcevo-Cris	Cris IIIA	Trench 1, Sector C, Square 1 and 2, oven	--

Radiocarbon Data: Tab.27 Cucuteni-Tripol'je

Lab-Code	14C-Age [BP]	δ13C [‰ PDB]	Material	Site	Grouped Phases	Period	Phase	Lat °N	Long °E	Reference
Bln-2087	5020 ± 60	--	--	Brinzeni 4	2	Tripol'je	T-B1	48,28	27,48	(1)
HD-14710	5360 ± 65	--	charcoal	Brinzeni 8	3	Tripol'je	T-B2	48,28	27,48	(1), (2)
HD-14898	4870 ±100	--	charcoal	Chapaevka	4	Tripol'je	T-C1	50,29	31,18	(1), (3)
Bln-2088	5390 ± 60	--	--	Cuconestii Vechi	2	Cucuteni	C-A3	47,99	27,18	(1)
HD-15024	5065 ± 19	--	bone	Cucuteni-Cetatuia	4	Cucuteni	C-B2	47,30	26,91	(4)
Bln-2137	5355 ±100	-	charcoal	Draguseni-Ostrov	2	Cucuteni	C-A3	48,01	26,80	(4)
Bln-2426	5205 ±100	--	charcoal	Draguseni-Ostrov	2	Cucuteni	C-A4	48,01	26,80	(4)
Bln-2428	5430 ±100	--	charcoal	Draguseni-Ostrov	2	Cucuteni	C-A4	48,01	26,80	(4)
HD-14761	5188 ± 18	--	bone	Draguseni-Ostrov	3	Cucuteni	C-A-B1	48,01	26,80	(4)
HD-14785	5246 ± 24	--	bone	Draguseni-Ostrov	3	Cucuteni	C-A-B1	48,01	26,80	(4)
HD-14791	4996 ± 26	--	bone	Draguseni-Ostrov	3	Cucuteni	C-A-B1	48,01	26,80	(4)
Bln-2429	5730 ± 50	--	charcoal	Drutsy 1	2	Tripol'je	T-B1	47,97	27,29	(8)
HD-15039	4790 ±100	--	--	Evminka 1	4	Tripol'je	T-C1	50,84	30,82	(1)
HD-15075	4890 ± 60	--	--	Evminka 1	4	Tripol'je	T-C1	50,84	30,82	(1)
Lv-2152	4615 ± 35	--	--	Gorodnytsya-Gorodyshche	5	Tripol'je	T-C2	46,95	29,76	(1)
Lv-2153	4615 ± 35	--	--	Gorods'k	5	Tripol'je	T-C2	50,89	29,59	(1)
Lv-2156	4499 ± 24	--	bone/human	Grumezoaia	5		H	--	--	(2)
Bln-2430	5340 ± 80	--	--	Habasesti-Holm	2	Cucuteni	C-A3	47,15	26,95	(4)
HD-15082	4938 ± 42	--	charcoal	Hancauti I	4	Cucuteni	C-B2	--	--	(2)
HD-15278	5127 ± 47	--	charcoal	Hancauti I	4	Cucuteni	C-B2	--	--	(2)
HD-15324	4884 ± 54	--	charcoal	Hancauti I	4	Cucuteni	C-B2	--	--	(2)
HD-15401	5106 ± 49	--	charcoal	Hancauti I	4	Cucuteni	C-B2	--	--	(2)
OxA-19840	4621 ± 95	--	charcoal	Hancauti I	5	Horodistea	H	--	--	(2)
OxA-22348	4495 ± 18	--	bone	Horodistea	5	Horodistea	H-1	49,28	31,45	(4)
UCLA-1466B	4235 ± 30	--	bone	Horodistea	5	Horodistea	H-2	49,28	31,45	(4)
UCLA-1642A	4377 ± 21	--	bone	Horodistea	5	Horodistea	H-2	49,28	31,45	(4)
Bln-2431	5345 ±100	--	grain/wheat	Leca-Ungureni	2	Cucuteni	C-A3	46,55	27,13	(4)
Hd-16700	4890 ± 60	--	charcoal	Maidanetskoe	4	Tripol'je	T-C1	48,79	30,68	(1)
Bln-2447	5420 ±150	--	charcoal	Malnas-Bai	2	Cucuteni	C-A2/A3	46,03	25,82	(2)
Bln-2480	4950 ±100	--	charcoal	Malnas-Bai	2	Cucuteni	C-A2/A3	46,03	25,82	(2)
Bln-2766	5940 ± 60	--	charcoal	Malnas-Bai	2	Cucuteni	C-A2/A3	46,03	25,82	(2)
Bln-2782	5490 ± 80	--	charcoal	Malnas-Bai	2	Cucuteni	C-A2/A3	46,03	25,82	(2)
Bln-2783	5880 ± 80	--	charcoal	Malnas-Bai	2	Cucuteni	C-A2/A3	46,03	25,82	(2)
Bln-2784	5497 ±100	--	charcoal	Malnas-Bai	2	Cucuteni	C-A2/A3	46,03	25,82	(4)
Bln-2802	5663 ± 42	--	charcoal	Malnas-Bai	2	Cucuteni	C-A2/A3	46,03	25,82	(4)
Bln-2803	5407 ± 20	--	bone	Malnas-Bai	2	Cucuteni	C-A2/A3	46,03	25,82	(4)
Bln-2804	5349 ± 40	--	bone	Malnas-Bai	2	Cucuteni	C-A2/A3	46,03	25,82	(4)
Bln-2805	5610 ± 55	--	grain/wheat	Margineni-Cetatuia	2	Cucuteni	C-A2	46,58	26,85	(4)
Bln-2824	5485 ± 60	--	grain/wheat	Margineni-Cetatuia	2	Cucuteni	C-A2	46,58	26,85	(4)
Bln-3191	5625 ± 50	--	charcoal	Margineni-Cetatuia	2	Cucuteni	C-A2	46,58	26,85	(4)
Bln-4598	5635 ± 50	--	charcoal	Margineni-Cetatuia	2	Cucuteni	C-A2	46,58	26,85	(4)
UCLA-1642B	4400 ±100	--	charcoal	Mayaki	5	Tripol'je	T-C2	46,69	30,93	(1), (3)
UCLA-1642F	4376 ± 60	--	--	Mayaki	5	Tripol'je	T-C2	46,69	30,93	(1)
UCLA-1642G	4375 ± 60	--	--	Mayaki	5	Tripol'je	T-C2	46,69	30,93	(1)
Hd-16701	5162 ± 37	--	bone	Mihoveni-Cahla Morii	4	Cucuteni	C-B1b	47,67	26,17	(4)
Hd-17930	4890 ± 29	--	bone	Mihoveni-Cahla Morii	4	Cucuteni	C-B2	47,67	26,17	(4)
Hd-17959	4904 ±300	--	--	Novo-Rozanovka	4	Tripol'je	T-C1	47,78	32,37	(1)
Bln-590	5565 ±100	--	charcoal	Novye Ruseshti 1	2	Tripol'je	T-B1	47,69	28,52	(1), (3)
Bln-1060	5780 ± 50	--	charcoal	Poduri-Dealul Ghindaru	1	Precucuteni	PC-3	46,48	26,53	(5)
Bln-1194	5880 ±150	--	grain/wheat	Poduri-Dealul Ghindaru	1	Precucuteni	PC-3	46,48	26,53	(5)
Bln-1195	5820 ± 50	--	charcoal	Poduri-Dealul Ghindaru	1	Precucuteni	PC-2	46,48	26,53	(5)

Radiocarbon Data: Tab.27

Lab-Code	14C-Age [BP]	δ13C [‰ PDB]	Material	Site	Grouped Phases	Period	Phase	Lat °N	Long °E	Reference
Bln-2087	5020 ± 60	--	--	Brinzeni 4	2	Tripol'je	T-B1	48,28	27,48	(1)
HD-14710	5360 ± 65	--	charcoal	Brinzeni 8	3	Tripol'je	T-B2	48,28	27,48	(1), (2)
HD-14898	4870 ±100	--	charcoal	Chapaevka	4	Tripol'je	T-C1	50,29	31,18	(1), (3)
Bln-2088	5390 ± 60	--	--	Cuconestii Vechi	2	Cucuteni	C-A3	47,99	27,18	(1)
HD-15024	5065 ± 19	--	bone	Cucuteni-Cetatuia	4	Cucuteni	C-B2	47,30	26,91	(4)
Bln-2137	5355 ±100	--	charcoal	Draguseni-Ostrov	2	Cucuteni	C-A3	48,01	26,80	(4)
Bln-2426	5205 ±100	--	charcoal	Draguseni-Ostrov	2	Cucuteni	C-A4	48,01	26,80	(4)
Bln-2428	5430 ±100	--	charcoal	Draguseni-Ostrov	2	Cucuteni	C-A4	48,01	26,80	(4)
HD-14761	5188 ± 18	--	bone	Draguseni-Ostrov	3	Cucuteni	C-A-B1	48,01	26,80	(4)
HD-14785	5246 ± 24	--	bone	Draguseni-Ostrov	3	Cucuteni	C-A-B1	48,01	26,80	(4)
HD-14791	4996 ± 26	--	bone	Draguseni-Ostrov	3	Cucuteni	C-A-B1	48,01	26,80	(4)
Bln-2429	5730 ± 50	--	charcoal	Drutsy 1	2	Tripol'je	T-B1	47,97	27,29	(8)
HD-15039	4790 ±100	--	--	Evminka 1	4	Tripol'je	T-C1	50,84	30,82	(1)
HD-15075	4890 ± 60	--	--	Evminka 1	4	Tripol'je	T-C1	50,84	30,82	(1)
Lv-2152	4615 ± 35	--	--	Gorodnytsya-Gorodyshche	5	Tripol'je	T-C2	46,95	29,76	(1)
Lv-2153	4615 ± 35	--	--	Gorods'k	5	Tripol'je	T-C2	50,89	29,59	(1)
Lv-2156	4499 ± 24	--	bone/human	Grumezoaia	5	Horodistea	H	--	--	(2)
Bln-2430	5340 ± 80	--	--	Habasesti-Holm	2	Cucuteni	C-A3	47,15	26,95	(4)
HD-15082	4938 ± 42	--	charcoal	Hancauti I	4	Cucuteni	C-B2	--	--	(2)
HD-15278	5127 ± 47	--	charcoal	Hancauti I	4	Cucuteni	C-B2	--	--	(2)
HD-15324	4884 ± 54	--	charcoal	Hancauti I	4	Cucuteni	C-B2	--	--	(2)
HD-15401	5106 ± 49	--	charcoal	Hancauti I	4	Cucuteni	C-B2	--	-	(2)
OxA-19840	4621 ± 95	--	charcoal	Hancauti I	5	Horodistea	H	--	--	(2)
OxA-22348	4495 ± 18	--	bone	Horodistea	5	Horodistea	H-1	49,28	31,45	(4)
UCLA-1466B	4235 ± 30	--	bone	Horodistea	5	Horodistea	H-2	49,28	31,45	(4)
UCLA-1642A	4377 ± 21	--	bone	Horodistea	5	Horodistea	H-2	49,28	31,45	(4)
Bln-2431	5345 ±100	--	grain/wheat	Leca-Ungureni	2	Cucuteni	C-A3	46,55	27,13	(4)
Hd-16700	4890 ± 60	--	charcoal	Maidanetskoe	4	Tripol'je	T-C1	48,79	30,68	(1)
Bln-2447	5420 ±150	--	charcoal	Malnas-Bai	2	Cucuteni	C-A2/A3	46,03	25,82	(2)
Bln-2480	4950 ±100	--	charcoal	Malnas-Bai	2	Cucuteni	C-A2/A3	46,03	25,82	(2)
Bln-2766	5940 ± 60	--	charcoal	Malnas-Bai	2	Cucuteni	C-A2/A3	46,03	25,82	(2)
Bln-2782	5490 ± 80	--	charcoal	Malnas-Bai	2	Cucuteni	C-A2/A3	46,03	25,82	(2)
Bln-2783	5880 ± 80	--	charcoal	Malnas-Bai	2	Cucuteni	C-A2/A3	46,03	25,82	(2)
Bln-2784	5497 ±100	--	charcoal	Malnas-Bai	2	Cucuteni	C-A2/A3	46,03	25,82	(4)
Bln-2802	5663 ± 42	--	charcoal	Malnas-Bai	2	Cucuteni	C-A2/A3	46,03	25,82	(4)
Bln-2803	5407 ± 20	--	bone	Malnas-Bai	2	Cucuteni	C-A2/A3	46,03	25,82	(4)
Bln-2804	5349 ± 40	--	bone	Malnas-Bai	2	Cucuteni	C-A2/A3	46,03	25,82	(4)
Bln-2805	5610 ± 55	--	grain/wheat	Margineni-Cetatuia	2	Cucuteni	C-A2	46,58	26,85	(4)
Bln-2824	5485 ± 60	--	grain/wheat	Margineni-Cetatuia	2	Cucuteni	C-A2	46,58	26,85	(4)
Bln-3191	5625 ± 50	--	charcoal	Margineni-Cetatuia	2	Cucuteni	C-A2	46,58	26,85	(4)
Bln-4598	5635 ± 50	--	charcoal	Margineni-Cetatuia	2	Cucuteni	C-A2	46,58	26,85	(4)
UCLA-1642B	4400 ±100	--	charcoal	Mayaki	5	Tripol'je	T-C2	46,69	30,93	(1), (3)
UCLA-1642F	4376 ± 60	--	--	Mayaki	5	Tripol'je	T-C2	46,69	30,93	(1)
UCLA-1642G	4375 ± 60	--	--	Mayaki	5	Tripol'je	T-C2	46,69	30,93	(1)
Hd-16701	5162 ± 37	--	bone	Mihoveni-Cahla Morii	4	Cucuteni	C-B1b	47,67	26,17	(4)
Hd-17930	4890 ± 29	--	bone	Mihoveni-Cahla Morii	4	Cucuteni	C-B2	47,67	26,17	(4)
Hd-17959	4904 ±300	--	--	Novo-Rozanovka	4	Tripol'je	T-C1	47,78	32,37	(1)
Bln-590	5565 ±100	--	charcoal	Novye Ruseshti 1	2	Tripol'je	T-B1	47,69	28,52	(1), (3)
Bln-1060	5780 ± 50	--	charcoal	Poduri-Dealul Ghindaru	1	Precucuteni	PC-3	46,48	26,53	(5)
Bln-1194	5880 ±150	--	grain/wheat	Poduri-Dealul Ghindaru	1	Precucuteni	PC-3	46,48	26,53	(5)
Bln-1195	5820 ± 50	--	charcoal	Poduri-Dealul Ghindaru	1	Precucuteni	PC-2	46,48	26,53	(5)
Bln-629	5350 ± 80	--	grain/wheat	Poduri-Dealul Ghindaru	2	Cucuteni	C-A2	46,48	26,53	(5)
Bln-631	5690 ± 50	--	charcoal	Poduri-Dealul Ghindaru	2	Cucuteni	C-A1	46,48	26,53	(5)
Bln-795	5680 ± 60	--	charcoal	Poduri-Dealul Ghindaru	2	Cucuteni	C-A1	46,48	26,53	(5)
BM-494	5420 ±150	--	charcoal	Poduri-Dealul Ghindaru	2	Cucuteni	C-A2	46,48	26,53	(4)
BM-495	5400 ± 70	--	charcoal	Poduri-Dealul Ghindaru	2	Cucuteni	C-A2	46,48	26,53	(4)
Gd-4682	5500 ± 60	--	charcoal	Poduri-Dealul Ghindaru	2	Cucuteni	C-A2	46,48	26,53	(4)
Gd-4685	5385 ± 37	--	grain	Poduri-Dealul Ghindaru	2	Cucuteni	C-A2	46,48	26,53	(4)
Gd-4690	5529 ± 29	--	charcoal	Poduri-Dealul Ghindaru	2	Cucuteni	C-A2	46,48	26,53	(4)
Gd-5858	5575 ± 35	--	charcoal	Poduri-Dealul Ghindaru	2	Cucuteni	C-A2	46,48	26,53	(4)
Gd-5860	5470 ± 90	--	bone/human	Poduri-Dealul Ghindaru	2	Cucuteni	C-A2	46,48	26,53	(8)
Gd-5861	5440 ± 70	--	charcoal	Polivanov Yar 3	2	Tripol'je	T-B1	48,67	27,67	(1)
Gd-6387	5423 ± 26	--	bone	Preutesti-Halta	2	Cucuteni	C-A3	47,45	26,41	(4)
Gd-6388	5595 ± 80	--	bone	Putineshti 3	2	Tripol'je	T-B1	47,96	28,02	(2)
GrN-1982	5379 ± 32	--	charcoal	Putineshti 3	2	Cucuteni	C-A4	47,96	28,02	(2)
GrN-1985	5520 ± 70	--	charcoal	Putineshti 3	2	Cucuteni	C-A4	47,96	28,02	(2)
Bln-1534	5700 ± 55	--	charcoal	Rogozhany 1	1	Precucuteni	PC-3	47,83	28,41	(5)
Hd-18678	4701 ± 42	--	bone	Sarata Monteoru	4	Cucuteni	C-B2	45,14	26,62	(2)
Hd-18826	4481 ± 33	--	bone	Sarata Monteoru	4	Cucuteni	C-B2	45,14	26,62	(2)
Hd-18936	4440 ± 25	--	bone	Sarata Monteoru	4	Cucuteni	C-B2	45,14	26,62	(2)
GrN-4424	5750 ±110	--	bone	Scanteia	2	Cucuteni	C-A3	46,90	27,58	(2)
GrN-5088	6320 ±110	--	bone	Scanteia	2	Cucuteni	C-A3	46,90	27,58	(2)
GrN-5099	5330 ±110	--	bone	Scanteia	2	Cucuteni	C-A3	46,90	27,58	(2)
GrN-5134	5388 ± 18	--	bone/human	Scanteia	2	Cucuteni	C-A3	46,90	27,58	(7)
HD-14109	5370 ± 26	--	bone/human	Scanteia	2	Cucuteni	C-A3	46,90	27,58	(7)
HD-14118	5345 ± 51	--	bone	Scanteia	2	Cucuteni	C-A3	46,90	27,58	(2)
HD-14544	5205 ± 63	--	bone	Scanteia	2	Cucuteni	C-A3	46,90	27,58	(2)
HD-14701	5280 ± 27	--	bone	Scanteia	2	Cucuteni	C-A3	46,90	27,58	(2)
HD-14792	4940 ± 95	--	--	Shkarovka	3	Tripol'je	T-B1-B2	49,48	30,53	(8)

Radiocarbon Data: Tab.27 (Cont.)

Lab-Code	14C-Age [BP]	δ13C [‰ PDB]	Material	Site	Grouped Phases	Period	Phase	Lat °N	Long °E	Reference
Hd-19373	5163 ± 36	--	charcoal	Sofia 8	4	Cucuteni	C-B1/B2	--	--	(2)
Hd-19419	4792 ±105	--	--	Soroki-Ozero	4	Tripol'je	T-C1	48,01	28,63	(1)
Hd-19426	4940 ±105	--	--	Soroki-Ozero	4	Tripol'je	T-C1	48,01	28,63	(1)
Hd-19441	4936 ± 40	--	--	Tal'yanki	4	Tripol'je	T-C1	48,80	30,53	(9)
Hd-19528	5048 ± 44	--	charcoal	Tal'yanki	4	Tripol'je	T-C1	48,80	30,53	(6)
Hd-19572	5032 ± 31	--	charcoal	Tal'yanki	4	Tripol'je	T-C1	48,80	30,53	(6)
BIn-1535	5830 ±100	--	bone	Targu Frumos	1	Precucuteni	PC-3	47,20	27,01	(5)
BIn-1536	5530 ± 85	--	charcoal	Tarpesti	1	Precucuteni	PC-3	47,16	26,45	(5)
BIn-1751	5700 ± 70	--	charcoal	Timkovo	1	Precucuteni	PC-3	48,10	29,29	(1),(8)
HD-14817	5165 ± 50	--	charcoal	Tsipleshty 1	3	Tripol'je	T-B2	47,82	28,14	(1),(8)
UCLA-1671B	4330 ± 60	--	--	Usatovo	5	Tripol'je	T-C2	46,53	30,65	(1)
Hd-19573	4950 ± 60	--	grain/wheat	Valea Lupului	4	Cucuteni	C-B2	47,18	27,50	(4)
IGAN-712	4990 ± 60	--	charcoal	Varvarovka 15	4	Tripol'je	T-C1	47,83	28,81	(1)
HD-14831	5180 ± 65	--	--	Veseliy Kut	3	Tripol'je	T-B1-B2	48,97	30,63	(8)

Reference

(1): Telegin et al., 2003
(2): Lazarovici 2010
(3): Quitta and Kohl, 1969
(4): Laszlo, 1997
(5): Mantu, 2000
(6) Rassamakin and Minotti, 2011
(7) Ivanova, 2008
(8) Luca and Suciu 2012
(9) Kruts 2008b